中国科研出版社
CHINA SCIENTIFIC RESEARCH PUBLISHING

Progress in Environmental Chemistry 2025, 1(1), 62.
https://doi.org/10.65746/pec62

Article

PM_{10} Hg aerosols and their variations due to emission sources and meteorological factors at three sites in Delhi city (India)

Anita Kumari, Umesh Chandra Kulshrestha*

School of Environmental Sciences, Jawaharlal Nehru University, New Delhi 110067, India
*** Corresponding author:** Umesh Chandra Kulshrestha, umeshkulshrestha@gmail.com

CITATION

Kumari A, Kulshrestha UC. PM_{10} Hg aerosols and their variations due to emission sources and meteorological factors at three sites in Delhi city (India). Progress in Environmental Chemistry. 2025; 1(1): 62. https://doi.org/10.65746/pec62

ARTICLE INFO

Received: 28 March 2025
Revised: 28 May 2025
Accepted: 10 June 2025
Available online: 26 June 2025

Abstract: Mercury air pollution is significantly harmful to human health. The first-ever detailed measurements of respirable-sized HgP levels were carried out at three sites in New Delhi in this study. The samples were collected at i) Jawaharlal Nehru University (JNU) (urban background site) and ii) Okhla (urban industrial cum residential site) during 2014–15, and iii) Badarpur (thermal power plant site) during January and February 2017, on quartz filters by using a high-volume air sampler. The mercury determination was carried out by using a VA computrace metal analyzer in differential pulse Anodic Stripping Voltammetry mode. The HgP levels varied from 0.24 to 1.43 ng m^{-3} with a mean of 0.74 ± 0.35 ng m^{-3} at JNU during the entire study period. At the Okhla site, the HgP levels varied from 0.19 to 7.36 ng m^{-3} with a mean of 1.40 ± 1.46 ng m^{-3}, while the HgP levels varied from 0.30 to 4.03 ng m^{-3} with a mean of 1.81 ± 0.96 ng m^{-3} at Badarpur during the winter season. HgP levels had significant spatio-temporal variations. The higher average concentrations of respirable HgP were observed during the winter season at all the sites as compared to the summer and monsoon seasons. Wind and pollution roses showed that the sampling sites were affected by local, regional, and transboundary pollution sources. Findings of this study will serve as an important reference for future assessment of atmospheric particulate mercury pollution in the Delhi National Capital Region. Anthropogenic HgP in the capital city of India still needs further long-term monitoring programs because of growing urbanization and industrialization.

Keywords: atmospheric mercury; voltammetry; particulate mercury; air pollution; meteorological parameters

1. Introduction

Mercury (Hg) is considered a global concern because of its global distribution through long-range transport even in remote areas, and studies on its presence in the environment are important due to its potential toxic impacts and bioaccumulation and biomagnification tendency, causing severe environmental and human health consequences [1–6]. Mercury is known to bioaccumulate in fatty tissues and biomagnify along the food chain in marine animals [3]. The harmful effects of Hg on human health are widely discussed in the literature and were first observed in Japan in 1956 [1]. The harmful effects of Hg on human health depend on types of Hg compounds and their exposure levels. Mercury in the atmosphere comes from natural sources, i.e., evaporation from soil, sediments, and water surfaces, forest fires, volcanoes, geothermal vents, etc., as well as anthropogenic sources, i.e., chlor-alkali, non-ferrous metals, cement production, waste incineration, coal combustion, electronics, plastic industries, etc. [4,7,8].

Typically, atmospheric Hg comprises three forms: particulate mercury (Hg_p or HgP), reactive gaseous mercury (Hg^{II} or RGM), and gaseous elemental mercury (GEM

or Hg^0). HgP consists of gaseous elemental or oxidized Hg species adsorbed or bound to atmospheric particles. These three forms of mercury are characterized based on the differences with respect to their atmospheric residence time, chemical and physical transformations, transport, deposition, and effect on ecosystems [9]. In the atmosphere, greater than 95 percent of the total mercury is present as GEM, which can undergo long-range transport because of its low reactivity, high stability, low water solubility, and long residence time (i.e., a few months to a year). However, RGM and HgP have short residence times and short-range transport because they have high scavenging coefficients, water solubility, reactivity, and dry deposition velocity as compared to GEM [10–12]. Quantification of Hg in particulate matter is of special relevance because, regardless of its lower concentrations (< 5% of total atmospheric Hg), atmospheric HgP plays a significant role in atmospheric Hg input or influx into aquatic and terrestrial ecosystems, therefore exerting influence on the global biogeochemical cycling of mercury [13–15].

Delhi's ambient air quality is deteriorating rapidly with time, particularly in the winter season. The sources of air pollution are heterogeneous and localized and highly dependent on season [16]. The combination of sources contributing to air pollution in Delhi includes industries, domestic combustion of biomass and coal, transport, thermal power plants, and municipal waste incineration [17]. Coal combustion, thermometer factories, steel industries, chlor-alkali industrial units, municipal waste incineration, and broken fluorescent lamps (CFLs), etc., are the most predominant sources of atmospheric Hg in India [18–21]. In India, because of increased industrial activities and coal combustion, the emissions of mercury into the atmosphere have also increased remarkably [18,20–22]. Extensive studies have been carried out worldwide on measurements of different forms of atmospheric mercury, but very limited studies have been carried out on mercury pollution in India, especially atmospheric mercury. However, studies on atmospheric mercury in Delhi are not available to date. Hence, in this study, we have aimed to report the temporal and spatial distribution of atmospheric HgP at three sites in New Delhi, India. Along with the influence of meteorological parameters on temporal and spatial variation of atmospheric HgP, the identification of the potential sources of atmospheric HgP at these sites was also investigated.

2. Methodology

2.1. Site descriptions

For this study, sampling was carried out at three sites, i.e., Jawaharlal Nehru University (JNU), Okhla, and Badarpur in New Delhi, India, as shown in **Figure 1**.

These sites differ in air pollution source types, population density, land use patterns, traffic density, and number of industrial sites. The major sources of air pollutants at these sites are vehicles, thermal power stations, industries, domestic burning (biomass), and waste incineration. The brief description of the sampling sites is given below.

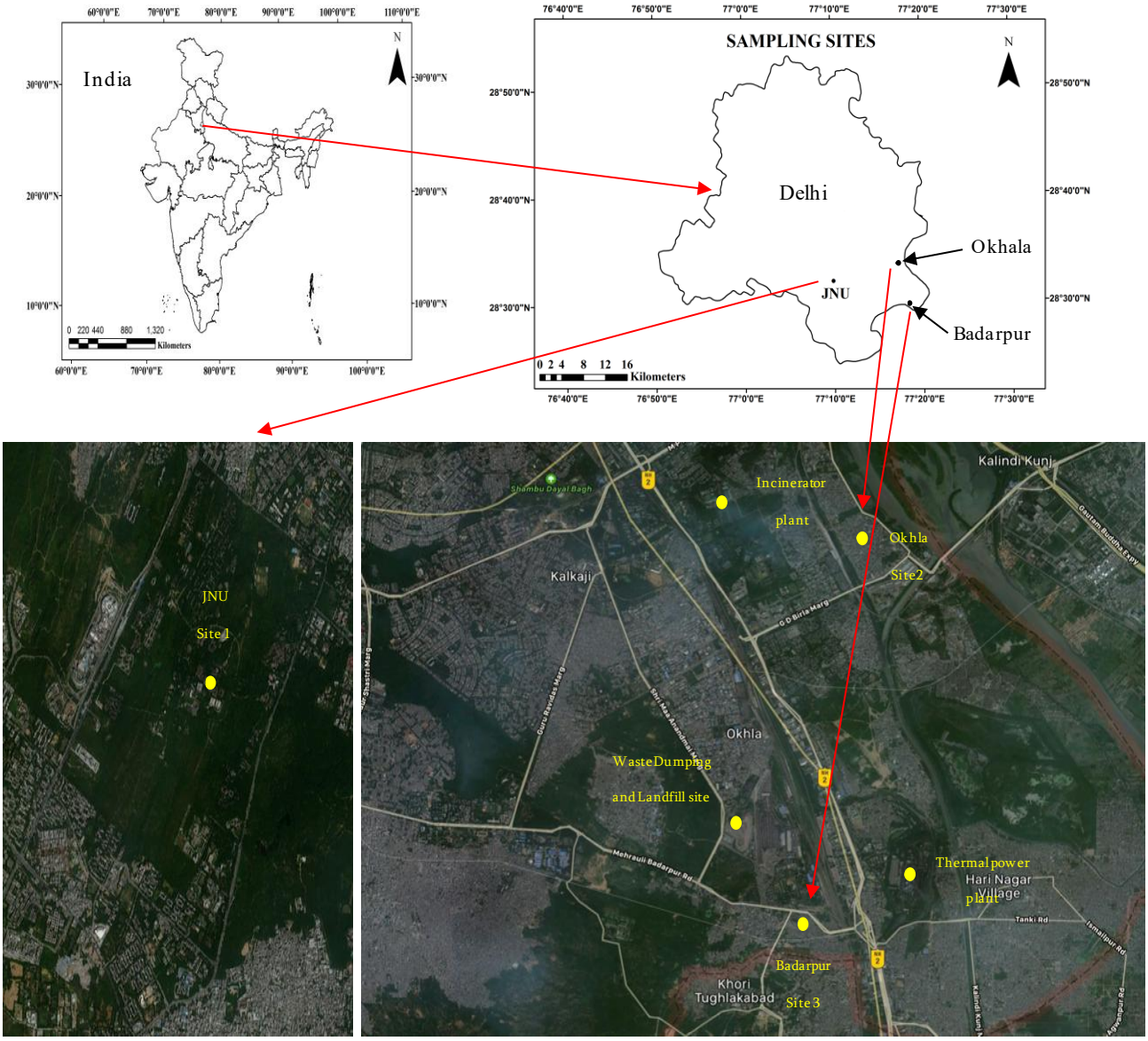

Figure 1. Location of the sampling sites.

2.1.1. Jawaharlal Nehru University

The JNU was selected as an urban background site in South Delhi (28°32′ N, 77°10′ E). The campus has extensive tree cover. There is no major industry located nearby or major pollution source within the JNU campus. However, in and around the campus, construction activities and vehicular traffic are important sources of air pollution. In addition, various residential colonies are situated near the campus, from where the air is moving over to JNU, affecting the air quality of the campus. Hence, at JNU, most of the atmospheric mercury associated with particulate matter is contributed by transport from other areas.

2.1.2. Okhla

Okhla was selected as an industrial-cum-residential urban site in Southeast Delhi (28°34′8.6″ N, 77°17′11″ E). The site is dominated by industries and heavy traffic. The site is congested in terms of roads, high-rise buildings, and other infrastructure.

In Okhla, air quality has been influenced by vehicular and industrial activities as well as waste incineration. There is an incinerator-based waste-to-energy plant in the proximity of the sampling site, which is using municipal waste as fuel and can also contribute hazardous pollutants like dioxins and heavy metals to the atmosphere. One of Delhi's landfill sites is also located in Okhla, emitting various pollutants into the atmosphere. Sampling was done at a residential site approx. 3 km away from waste-to-energy incinerator plant.

2.1.3. Badarpur

Badarpur was selected as an industrial-cum-residential urban site in South Delhi (28°30′14.3″ N, 77°18′6.5″ E). The site is also dominated by industries and heavy traffic. One of the coal-based thermal power plants (TPPs) of the National Thermal Power Corporation (NTPC), with an installed capacity of 720 MW, was located in this locality. It was one of the oldest TPPs that supplied power to Delhi. However, the plant which was in operation till recently has been shut down due to the continuously deteriorating air quality of Delhi. Sampling was carried out at the residential site near Badarpur border approx. 1.5 km away from this plant. Waste dumping and landfill sites are also located near the sampling site.

2.2. Samples collection

At the JNU site, samples were collected during August–September 2014, December 2014–February 2015, and May 2015. At the Okhla site, samples were collected during October–November 2014, and August 2015. At Badarpur, samples were collected during January–February 2017. Samples collected during March to June are termed "summer samples", samples collected during July–October are termed "monsoon samples", while samples collected during November–February are termed "winter samples". Sample collection was done on the rooftop of a four-story building (~20 m height), a one-story building (~5 m height), and the School of Environmental Science (SES) building (~20 m height) at Okhla, Badarpur, and JNU campus, respectively. Sampling was done on quartz filters (Grade QM-A, Whatman) by using a high-volume Respirable Dust Sampler (RDS, AAS 217BL Model, Ecotech) having a 10 μm particulate cutoff diameter. The flow rate for sampling was 0.88–1.25 m^3 min^{-1}. The average sampling duration was 24 h to accumulate a sufficient mercury amount for quantification. Prior to sampling, the filters were combusted for 1 h at 450 °C and then equilibrated for 24 h in a desiccator and then weighed. Note down the initial weight of the filters. After sampling, the samples were handled, and transported to the laboratory by using the same procedure as described by Morton-Bermea [23] and Kumari and Kulshrestha [24]. In the laboratory, filters were again equilibrated for 24 h in the same desiccator and then weighed to note down the final weight of the filters [25]. The mass concentration of PM_{10} collected on each filter was estimated by using the initial and final weights of the filter. All the samples were preserved in airtight boxes at −18 °C (in the freezer of the refrigerator) till analysis. During all the above-mentioned steps, particle-free gloves were worn to avoid contamination.

The losses of Hg from the filters, especially during the summer season, may take place during the above-mentioned steps (i.e., sample collection, sample handling, and equilibration process). Therefore, the concentrations reported here might be

underestimated. But, in order to minimize such artifacts and the relative error in sample collection and analysis, precautions were taken and all samples were carefully handled in the same way. The field blanks were also analyzed by using the same method as used for samples. A total of 28, 28, and 14 samples were collected at JNU, Okhla, and Badarpur sites, respectively. However, at Okhla, during winter season, out of 13 samples only 10 samples were used for data interpretation due to insufficient volume of extracted samples. Therefore, to match the matrix, out of total 28 samples only 25 samples were used for final calculations at Okhla.

2.3. Sample preparation

For the analysis, one-fourth portion of the filters (PM_{10} samples) was extracted in 50 mL of five percent HNO_3 by holding in an ultrasonic water bath for 60 min [24,26]. The extracted solution was filtered through nylon syringe filters (pore size 0.22 μm) and stored in polypropylene bottles (rigorously washed with 5% HNO_3 prior to use in order to avoid adsorption of metals on these bottles) in a refrigerator (4 °C) until analysis. In order to find out the efficiency of the first extraction, the blank and 3 samples were extracted again after the first extraction by using the same procedure as mentioned above and analyzed. Prior to use, all the sample containers and glassware were thoroughly acid-cleaned.

2.4. Mercury determination

Mercury measurements were carried out by using a 797 VA Computrace analyzer (Version 1.3.2.85, Metrohm, Switzerland) in Differential Pulse Anodic Stripping Voltammetry (DPASV) mode. Various researchers have widely used different modes of voltammetry techniques for mercury and other heavy metals determination in various kinds of environmental samples [24,27–33]. In previous studies, the results obtained by the Anodic Stripping Voltammetry (ASV) were compared with different analytical methods such as Cold Vapor Atomic Absorption Spectrometry [28], Inductively Coupled Plasma-Atomic Emission Spectrometry, and Inductively Coupled Plasma-Mass Spectrometry [29] and found to be in good agreement, and results were not significantly different. Therefore, Anodic Stripping Voltammetry is a reliable, highly sensitive, fast, easy-to-use, and affordable alternative to costly analytical techniques [28,29].

An Ag/AgCl/KCl (3 mol L^{-1}) electrode, glassy carbon electrode, and Gold-Rotating Disk Electrode (Au-RDE) (2 mm diameter) were used as reference electrode, auxiliary electrode, and working electrode, respectively. Before use, the Au-RDE working electrode was cleaned and conditioned extensively as described by Metrohm [34] and Kumari and Kulshrestha [24]. Certified Reference Materials (CRM) (mercury nitrate ($Hg(NO_3)_2$) in nitric acid) from the National Institute of Standards and Technology were used as stock solution (1000 ppm or mg L^{-1}) from which working standards of mercury (10 ppb or μg L^{-1} and 1 ppm or mg L^{-1}) were prepared. The primary or electrolyte solution taken in Voltametric Cell (VC) contained Ethylenediaminetetraacetic acid (EDTA) (0.1 molar), perchloric acid (70% ACS), and KCl (3 mol L^{-1}).

In the DPASV technique, the analysis is carried out in two steps, i.e., deposition

and stripping steps. In the deposition step, the analyte to be measured gets deposited on the Au-RDE working electrode at a constant deposition potential (0.037 V), which continues up to a deposition time of 260 s. In the stripping step, the analyte deposited on the Au-RDE working electrode is dissolved back into the solution. In the stripping step, the potential is scanned (between 300 and 840 mV) at a certain rate (0.02 V s^{-1}), and the generated current is measured.

For Hg analysis, 10 mL of extracted sample, 400 μL of EDTA solution, 100 μL of KCl, and 300 μL of perchloric acid were pipetted out into the VC and purged for 300 s with pure N_2 gas in order to remove the dissolved O_2 and then, using the above-mentioned voltammetry parameters, voltammograms were registered. After that, 200 μL of 1 mg L^{-1} mercury standard solution was added into the VC, and corresponding voltammograms were obtained for the first addition of standard, and then 200 μL of 1 mg L^{-1} mercury standard solution was again added into the VC, and corresponding voltammograms were obtained for the second addition of standard [24]. The mercury concentration was determined by peak height. The 521 mV was the peak potential for mercury. The detailed procedure of this method is described elsewhere [24]. For preparation of all solutions, ultrapure water (Milli-Q) was used.

2.5. Trace metal determination

Mn, Zn, Ni, Fe, Pb, Cd, Co, Cr, Cu, Ca, Na, Mg, and K were also determined in the extracted aerosol samples by using an Atomic Absorption Spectrometer (AAS) (Thermo Electron Corporation, model M6, USA). Single-element standards of E-Merck were used for calibration of AAS. Working standards of required concentrations were prepared by serial dilution of the stock solution of the higher concentration of 1000 ppm by using Milli-Q water. The data precision was observed by analyzing the standards at regular intervals during analysis. All the elements investigated were determined by using an atomizer with an air/acetylene burner. All instrumental settings used during analysis were those recommended in the manual. Co was found below detection in all the samples.

2.6. Statistical analysis

Statistical analyses were done by using SPSS (version 16), and graphs, wind rose, and pollution roses were plotted with the help of Origin (versions 8 and 24). The Pearson's correlation coefficient was done to identify the relationship between mercury and weather conditions and trace elements.

Quality control/quality assurance: Method blanks, field blanks, and reagent blanks were frequently analyzed in order to evaluate precision and analytical bias and to determine the contribution of reagents to the concentration of mercury obtained for the samples. The standard addition method was used for quantitative measurement of Hg, and calibration methods were used for trace metal determination. The readings of field blank samples were taken into account while calculating the final values of samples. CRM of mercury (mercury nitrate ($Hg(NO_3)_2$) in nitric acid) from the National Institute of Standards and Technology (NIST) was used to check the accuracy and precision of analytical determination of mercury. The analytical precision was found to be 4.6% for mercury, which was measured by taking the relative standard

deviation of triplicate readings of a sample. Extraction efficiency of mercury in the first extraction was found to be very high (i.e., 97% to 99%).

3. Results and discussion

3.1. Levels of PM_{10} mercury (HgP) in the atmosphere

At JNU, the atmospheric HgP levels varied from 0.24 to 1.43 ng m^{-3} with an average of 0.74 ± 0.35 ng m^{-3} and a median of 0.75 ng m^{-3} during the whole study period. During monsoon, the HgP levels varied from 0.25 to 0.94 ng m^{-3} with an average of 0.54 ± 0.24 ng m^{-3}, and during summer, the HgP levels varied from 0.24 to 1.18 ng m^{-3} with an average of 0.77 ± 0.31 ng m^{-3}, while the HgP levels varied from 0.32 to 1.43 ng m^{-3} with an average of 0.91 ± 0.37 ng m^{-3} during the winter season at JNU (**Table 1**).

Table 1. Statistical summary of atmospheric HgP levels (ng m^{-3}) at JNU, Okhla, and Badarpur during different seasons.

Site	Season	Minimum	Maximum	Median	Mean ± SD
JNU	Monsoon 2014 (*N* = 8)	0.25	0.94	0.47	0.54 ± 0.24
	Winter 2014–15 (*N* = 11)	0.32	1.43	0.98	0.91 ± 0.37
	Summer 2015 (*N* = 9)	0.24	1.18	0.78	0.77 ± 0.31
Okhla	Winter 2014 (*N* = 13)	0.40	7.36	1.80	2.33 ± 1.94
	Monsoon 2015 (*N* = 15)	0.19	1.73	0.61	0.79 ± 0.48
Badarpur	Winter 2017 (*N* = 14)	0.30	4.03	1.99	1.81 ± 0.96

N: Number of samples; SD: Standard deviation.

At Okhla, the concentrations of atmospheric HgP varied from 0.19 to 7.36 ng m^{-3} with an average of 1.40 ± 1.46 ng m^{-3} and a median of 0.96 ng m^{-3} during the whole study period. During winter, the HgP levels varied from 0.40 to 7.36 ng m^{-3} with an average of 2.33 ± 1.94 ng m^{-3}, while the HgP levels varied from 0.19 to 1.73 ng m^{-3} with an average of 0.79 ± 0.48 ng m^{-3} during monsoon season at Okhla (**Table 1**). At Badarpur, atmospheric HgP was measured during the winter season only. During the winter season, atmospheric HgP levels varied from 0.30 to 4.03 ng m^{-3} with an average of 1.81 ± 0.96 ng m^{-3} and a median of 1.99 ng m^{-3} at Badarpur (**Table 1**), showing that the HgP concentration varied over a wide range.

The average concentration of atmospheric HgP was recorded highest during the winter season, followed by summer, and lowest during the monsoon season at JNU. However, at JNU, atmospheric HgP concentrations did not show significant seasonal variations. The possible reason for lesser seasonal variation of atmospheric HgP at JNU could be the absence of significantly active sources of mercury, and therefore, no significant accumulation of HgP during seasonal variations in meteorological conditions. However, in the absence of significantly active sources of mercury at JNU, seasonal variations in meteorological factors, i.e., ambient temperature, precipitation, humidity, and wind speed and direction, could have influenced the concentrations of HgP [35–38].

The approx. concentration of atmospheric HgP at Okhla was higher during the

winter season as compared to the monsoon season, indicating higher emissions and less dispersion and deposition during winters. However, as compared to JNU, atmospheric HgP concentrations had more pronounced seasonality or significant seasonal variations at Okhla. The possible sources of HgP at Okhla include industries, municipal waste incineration, traffic, residential combustion (biomass burning), etc. At Okhla, one of the reasons for high HgP levels during winters could be waste incineration, as an incinerator-based waste-to-energy plant was located near the residential colony where the sampling was carried out. Incinerators release many harmful chemicals into the atmosphere. In the waste incinerator, combustion of Hg-containing products such as CFLs, fluorescent tubes, thermometers, thermostats, batteries, and other products that are discarded in municipal solid waste (MSW) as household waste contributes Hg to flue gas and fly ash. In the waste incinerator, Hg and its compounds are volatile at combustion temperatures; therefore, most of the Hg in the waste feed is vaporized during incineration in the combustion chamber [39,40]. Therefore, HgP concentrations at Okhla might have been affected by variations in emission intensity of the sources and meteorological factors, i.e., precipitation, humidity, wind speed and direction, and temperature, as described in Section 3.5 [25,35–38,41,42].

At Badarpur, atmospheric HgP during the sampling period (i.e., the winter season only) varied over a wide range, and the possible sources of atmospheric HgP might be industries, traffic, and residential combustion, as well as coal combustion in thermal power plant (TPP) as one of the NTPC's TPP was located near the residential colony where sampling was carried out. Up to 8% of the ambient particulate matter pollution in Delhi can be attributed to the coal-fired TPPs of capacity 2000 MW operating within a 60 km radius from the city's center [43].

The possible reasons for higher HgP levels during winters might be favorable local meteorological conditions (i.e., decreased mixing heights, temperature inversion, and less precipitation, which are prevalent incidences during the winter season) resulting in the accumulation of particulate matter in the atmosphere, which could not disperse or dilute easily, as well as continuously enhanced emissions from existing sources (anthropogenic or natural or both). The higher HgP levels in winters might also be due to combustion because particulate matter levels would rise with a rise in combustion activity [44,45] and increased particle levels would accordingly possess more space to adsorb or trap gas-phase Hg species and thus increase the HgP levels. The lower temperature in winters would further enhance adsorption of gas-phase mercury on the particulate matter as described in Section 3.5.1. Another reason for higher HgP levels during winters might be local, regional, and long-range transportation, as suggested in Section 3.5.3. As explained in Section 3.5.3, the contribution from local sources or direct emission from the active sources as compared to transported HgP was responsible for higher atmospheric HgP at Okhla and Badarpur.

At JNU, the lower HgP levels during summer could be due to enhanced mixing heights resulting in dispersion or dilution of particulate matter and desorption of mercury from particles to air because of higher temperatures in the summer season, as described in Section 3.5.1. During monsoon, the lowest HgP levels at JNU and lower levels at Okhla might be due to the scavenging effect (wet deposition) of rain events,

as some light to heavy rainfall events were noticed during the monsoon season sampling, and lower HgP levels were recorded in samples collected after rainfall events.

3.2. Comparison of atmospheric HgP levels at these sites

The higher average concentrations of atmospheric HgP were observed during the winter season at all the sites. The highest concentration of atmospheric HgP was observed at Okhla during winters, then at Badarpur during winters, and then at JNU during winters (**Figure 2**), suggesting the particulate matter build-up in the lower atmosphere because of favorable local meteorological conditions at JNU, Okhla, and Badarpur, as well as continuously enhanced emissions or release from existing sources, especially at Okhla and Badarpur.

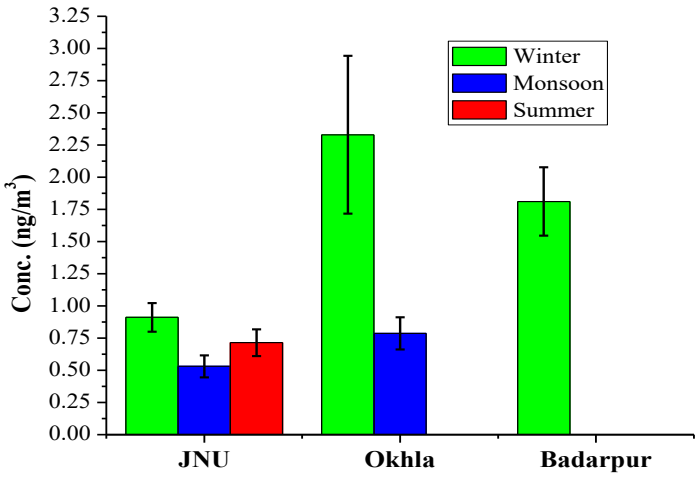

Figure 2. Comparison of atmospheric HgP concentrations at JNU (winter, monsoon, and summer), Okhla (winter and monsoon), and Badarpur (winter) during different seasons.

The higher concentrations of atmospheric HgP at Okhla and Badarpur were recorded possibly because of the dominance of industrial and vehicular activities, as well as some site-specific activities at these sites. The lowest concentration of atmospheric HgP was observed at JNU during monsoon. The higher concentration of atmospheric HgP at Okhla even during monsoon as compared to JNU during summer and monsoon indicates significantly active sources of mercury at Okhla. Therefore, significant differences in atmospheric HgP levels at all these sites may be attributed to differences in types of sources and their emission intensity, meteorological parameters, and month of the year in which sampling was carried out.

3.3. Comparisons with other worldwide studies

Comparison of the present study with worldwide studies was done as shown in **Table 2**. On average, atmospheric HgP concentrations at JNU, Okhla, and Badarpur were very low in comparison to other studies reported from India, which were carried out in the middle of the industrial belts, having very high-intensity multiple sources of mercury such as integrated steel plants, thermometer manufacturing industries, metallurgical units, fertilizer factories, caustic soda factories, chloralkali plants, TPPs,

etc. At those sites, the average HgP concentrations were approx. 20 to 2000 times higher as compared to average HgP concentrations at our sampling sites (**Table 2**). The global comparison shows that the HgP levels at JNU, Okhla, and Badarpur were significantly higher than most cities in Europe and North America, and were approx. comparable to the values reported from most of the sites in Asia. But, it should be noted that in the present study, the HgP levels were measured in PM_{10}, while in most of the other studies, HgP levels were measured in $PM_{2.5}$, except few sites. These differences observed in HgP levels might be due to different sampling site characteristics, emission strength of sources, and the size of the collected particles.

Table 2. Comparison of atmospheric HgP at JNU, Okhla, and Badarpur and other studies around the world.

Location	Site type	Period	Cutoff size	HgP (pg m^{-3})	Reference
JNU, Delhi, India	Urban	August 2014–May 2015	PM_{10}	0.74 ± 0.35*	Present study
Okhla, Delhi, India	Urban	October 2014–August 2015	PM_{10}	1.40 ± 1.46*	Present study
Badarpur, Delhi, India	Urban	January–February 2017	PM_{10}	1.81 ± 0.96*[a]	Present study
Mahasar, India	Rural	December 2014–June 2015	PM_{10}	756.7 ± 436.3	[24]
Tuticorin, India	Industrial	-	PM_{10}	20 ± 10*	[20]
Bhilai, India	Industrial	March 2005–February 2006	PM_{10}	2.27-24.37**	[21]
Tamil Nadu, India	Industrial	-	PM_{10}	580 ± 760*	[46]
Kathmandu, Nepal	Suburban	April 2013–April 2014	TSP	850.5 ± 926.8	[42]
Lumbini, Nepal	Urban	April 2013–July 2014	TSP	99.7 ± 92.6	[47]
Shanghai, China	Urban	July 2004–May 2007	TSP	560 ± 220	[48]
Beijing, China	Urban	January 2003–October 2004	TSP	1180 ± 820	[49]
Nyingchi, China	Rural	March 2019–September 2019	$PM_{2.5}$	9.3 ± 5.9	[50]
Hefei, China	Suburban	February–May 2009	TSP	320 ± 100	[51]
Jinan, China	Suburban	June 2014–December 2015	$PM_{2.5}$	508.5 ± 402.7	[25]
Xiamen, China	Coastal	March 2012–February 2013	$PM_{2.5}$	174.4 ± 280.6	[52]
Lhasa, China	Urban	August 2016–February 2017	$PM_{2.5}$	54.5 ± 119.5	[53]
Nanjing, China	Urban	June 2011–February 2012	PM_{10}	1100 ± 570	[54]
Huaniao Island, China	Island	March 2012–January 2013	TSP	230 ± 150	[55]
Lhasa, China	Urban	April 2013–August 2014	TSP	224 ± 139	[41]
Seoul, Korea	Urban	February 2005–February 2006	$PM_{2.5}$	23.9 ± 19.6	[56]
Seoul, Korea	Urban	December 2009–July 2010	TSP	6.8 ± 6.5	[57]
Seoul, Korea	Urban	2007–2008	TSP	65.4 ± 47.8	[58]
Seoul, Korea	Urban	2006–2009	$PM_{2.5}$	13.4 ± 12.0	[59]
Chuncheon, Korea	Rural	2006–2009	$PM_{2.5}$	3.7 ± 5.7	[59]
Tokyo, Japan	Urban	April 2000–March 2001	PM_{10}	98 ± 51	[36]
Cape Hedo, Japan	Remote	March–May 2004	$PM_{2.5}$	3.0 ± 2.5	[60]
Zabrze, Poland	Urban	October 2006–April 2007	$PM_{2.5}$	100.4	[61]
Zabrze, Poland	Urban	January–December 2013	TSP	65.5 ± 53.7	[62]
Zabrze, Poland	Urban	January–December 2013	PM_{10}	63.6 ± 53.0	[62]
Lichwin, Poland	Suburban	August 2003	TSP	110 ± 50	[63]
Lichwin, Poland	Suburban	January–February 2004	TSP	1050 ± 180	[63]

Table 2. (*Continued*).

Location	Site type	Period	Cutoff size	HgP (pg m^{-3})	Reference
Göteborg, Sweden	Urban	February 2005	$PM_{2.5}$	12.5 ± 5.88	[64]
Waldhof, Germany	Rural	2009–2011	$PM_{2.5}$	6.3	[65]
Novembera Scotia, Canada	Urban	January 2010–December 2011	$PM_{2.5}$	2.3 ± 3.1	[66]
Toronto, Canada	Urban	December 2003–November 2004	$PM_{2.5}$	21.5 ± 16.4	[67]
Mexico City	Urban	March 2006	$PM_{2.5}$	187 ± 300	[68]
Mississippi, USA	Urban	July 2011–June 2012	$PM_{2.5}$	4.58 ± 3.40	[69]
Chicago, USA	Urban	July–November 2007	$PM_{2.5}$	9 ± 20	[70]
Detroit, USA	Urban	January–December 2003	$PM_{2.5}$	20.8 ± 30.0	[71]
Thompson Farm, USA	Coastal	February 2009–August 2010	$PM_{2.5}$	0.19–1.14	[72]
East St Louis, USA	Urban	October–December 2002	$PM_{2.5}$	483 ± 1954	[73]
Rochester, USA	Suburban	December 2007–November 2009	$PM_{2.5}$	8.7 ± 12.8	[74]
São Paulo State, Brazil	Urban	2002–2003	TSP	400 ± 300	[75]
Kodaikanal, India	Remote	January 2015–December 2016	-	1.53*[b]	[76]
Chennai, India	Urban	January 2015–December 2016	-	4.68*[b]	[76]
Kanpur, India	Urban	January 2007–January 2008	PM_{10}	776.4 ± 845.5	[77]

* ngm^{-3}; ** μgm^{-3}; [a] Winter season only; [b] Total Gaseous Mercury (TGM).

3.4. HgP to PM_{10} mass ratio (HgP/PM_{10}) and correlation between HgP and PM_{10}

At JNU, the HgP/PM_{10} ratio varied from 1.24 to 7.28 μg g^{-1} with an average of 4.48 ± 1.71 μg g^{-1} (**Table 3**). At Okhla, the HgP/PM_{10} ratio varied from 0.84 to 10.87 μg g^{-1} with an average of 5.11 ± 3.01 μg g^{-1}, while at Badarpur, it varied from 1.07 to 9.04 μg g^{-1} with an average of 6.3 ± 2.48 μg g^{-1} (**Table 3**).

Table 3. Statistical summary of atmospheric HgP to PM_{10} mass ratio (HgP/PM_{10}) (μg g^{-1}) at JNU, Okhla, and Badarpur.

Sites	Minimum	Maximum	Median	Mean ± SD
JNU	1.24	7.28	4.32	4.48 ± 1.71
Okhla	0.84	10.87	4.08	5.11 ± 3.01
Badarpur	1.07	9.04	5.36	6.30 ± 2.48

In Indian coal, Hg content varies from 0.18 to 0.61 μg g^{-1}. According to Koshle et al. [78], average Hg content in soil ranged from 3.59 to 16.58 μg g^{-1} at various locations near an integrated steel plant in Bhilai, but these sites were highly polluted with Hg. A study by Supriti et al. [79] found mercury concentrations in soil around a coal-fired thermal power plant in India less than or similar to those observed in India or other parts of the world (2.4–40.2 μg/kg). Another study by Bhave et al. [80] reported total mercury (THg) concentrations in topsoil samples in the range of 64.60–2189.30 μg kg^{-1} and 3.88–1209.93 μg kg^{-1} at two municipal solid waste dumping sites in Mumbai, India. The information on Hg content in soil and atmospheric HgP levels at Delhi, as well as HgP to PM_{10} ratios in India, is not available. However, average values of HgP to PM_{10} ratios were significantly high at these sites as compared to the

values observed at other cities abroad, such as 1.4 μg g^{-1} in Beijing [15], 0.18 μg g^{-1} in Seoul [57], and 2.59 μg g^{-1} in Kathmandu [42]. The higher Hg mass content in PM_{10} indicated significant enrichment of mercury on PM_{10}, and therefore suggested its contribution most likely came from anthropogenic sources.

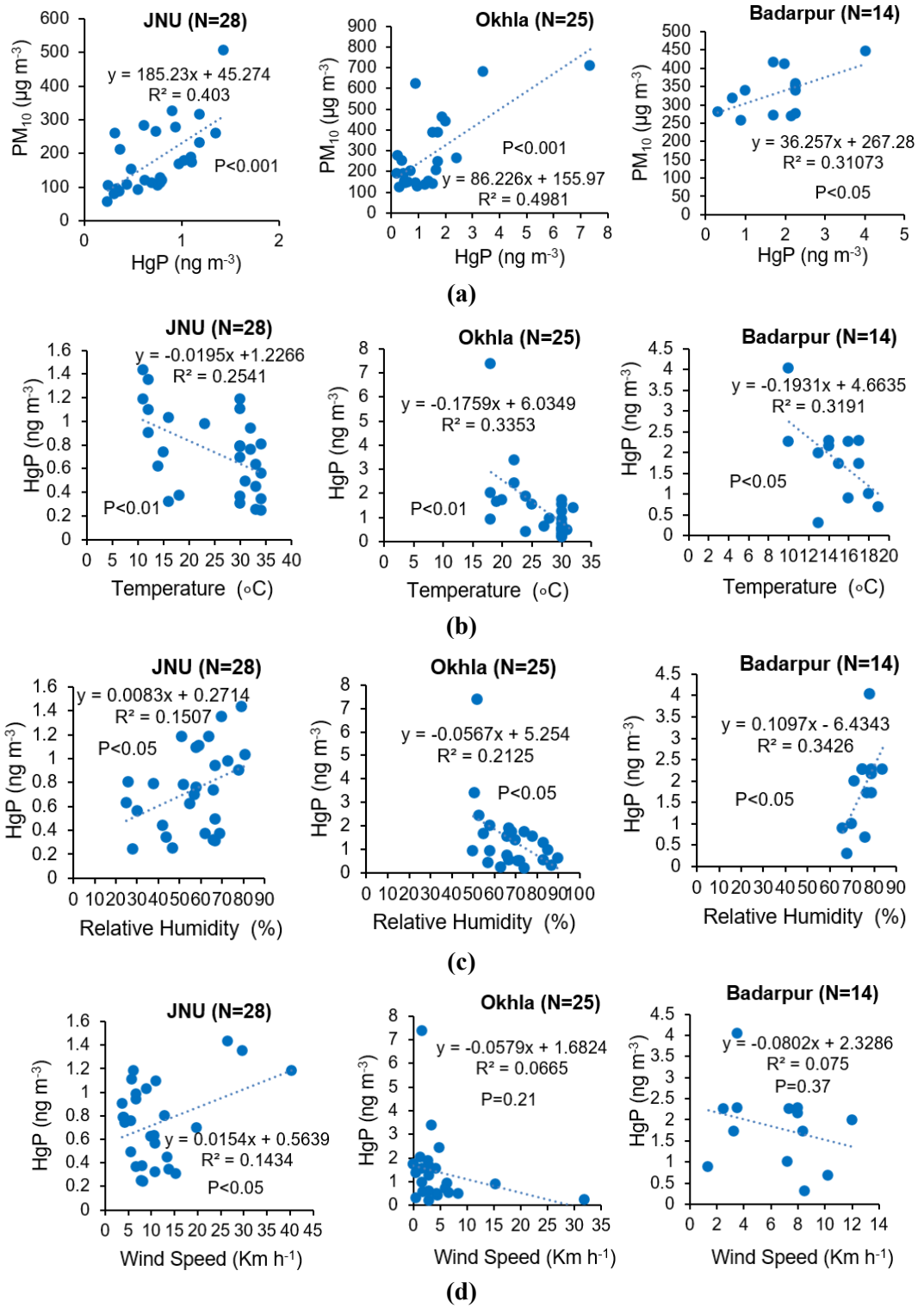

Figure 3. (a) Regression plots between HgP and PM_{10}; **(b)** HgP and temperature; **(c)** HgP and relative humidity;**(d)** HgP and wind speed at JNU, Okhla, and Badarpur (*N*: Number of samples).

The regression analysis, as well as Pearson's correlation analysis between HgP and PM10, was also attempted at all these sites. **Figure 3a** shows a regression plot between HgP and PM10 at JNU, Okhla, and Badarpur. The Pearson's correlation coefficient between HgP concentration and PM10 at JNU, Okhla, and Badarpur are given in **Table 4**.

Table 4. Pearson's correlation coefficient between HgP concentration and meteorological factors at JNU, Okhla, and Badarpur.

	HgP	**Temperature**	**Humidity**	**Wind speed**	**PM_{10}**
JNU					
HgP	1				
Temperature	**−0.50****	1			
Humidity	**0.39***	**−0.67****	1		
Wind Speed	**0.38***	**−0.40***	0.14	1	
PM_{10}	**0.58****	**−0.70****	**0.52****	0.28	1
Okhla					
HgP	1				
Temperature	**−0.58****	1			
Humidity	**−0.46***	**0.66****	1		
Wind Speed	−0.26	0.23	−0.23	1	
PM_{10}	**0.71****	**−0.77****	**−0.68****	−0.08	1
Badarpur					
HgP	1				
Temperature	**−0.57***	1			
Humidity	**0.59***	−0.29	1		
Wind Speed	−0.27	−0.02	0	1	
PM_{10}	0.28	0.15	0.01	−0.12	1

** Correlation is significant at the 0.01 level (2-tailed).
* Correlation is significant at the 0.05 level (2-tailed).

The Pearson's correlation (**Table 4**) between PM_{10} and HgP concentration indicated that HgP and PM_{10} were significantly positively correlated at JNU (r^2 = 0.403, $P < 0.001$), Okhla ($r^2 = 0.498$, $P < 0.001$), and Badarpur ($r^2 = 0.311$, $P < 0.05$). It is illustrated in the regression plot (**Figure 3a**) too. The statistically significant positive correlation between PM_{10} and HgP suggested that PM_{10} and HgP had been contributed either from the same or similar sources or GEM or gaseous Hg^{2+} got adsorbed onto existing particulate matter in the same air mass prior to their (air masses) arriving at these sampling sites [10]. Hence, in Delhi, the higher HgP levels were mainly influenced by an increase in both the HgP/PM_{10} ratio and PM_{10} simultaneously.

3.5. Influence of meteorological parameters on atmospheric HgP levels

The previous studies have suggested that the temporal and spatial variation of HgP levels could be influenced by variation in emission intensity of sources and meteorological factors, i.e., humidity, rainfall, wind speed and direction, solar radiation, and temperature [25,35–38,41,42]. As shown in **Figure 2**, there were clear

and noticeable temporal and spatial variations in HgP levels at Delhi, with higher HgP levels during the winter season (highest at Okhla) and lower HgP levels during the summer season and lowest HgP levels during the monsoon season (lowest at JNU). As explained in Sections 3.1 and 3.2, the study sites (JNU, Okhla, and Badarpur) have some site-specific activities that are responsible for variations in HgP concentrations. Therefore, we can conclude that variations of HgP levels were influenced by HgP emissions intensity of anthropogenic sources and meteorological factors. To find out the influence of meteorological parameters on atmospheric HgP level, the relationship between atmospheric HgP level and meteorological factors, i.e., relative humidity, wind speed and direction, temperature, and precipitation, was examined, and the Pearson's correlation coefficient and regression plot between HgP level and meteorological factors were calculated at JNU, Okhla, and Badarpur, as shown in **Table 4** and **Figure 3**, respectively.

3.5.1. Influence of temperature on atmospheric HgP levels

The photochemical conversion and gas-particle phase partition coefficient of Hg species play a significant role in the formation of particulate mercury (HgP) in the atmosphere [48,81,82]. The HgP comprises gaseous elemental Hg and gaseous Hg^{2+} which are adsorbed onto the particle surface. The gas-particle phase partitioning of mercury species is highly influenced by temperature, and hence, the adsorption of gaseous elemental Mercury and gaseous Hg^{2+} onto the particle surface is more efficient at low temperatures, because with a decrease in temperature, the partitioning coefficient increases [38,82].

The Pearson correlation coefficient (**Table 4**) between temperature and HgP levels showed a significantly negative correlation at JNU ($r^2 = 0.254$, $P < 0.01$), Okhla ($r^2 = 0.335$, $P < 0.01$), and Badarpur ($r^2 = 0.371$, $P < 0.05$). It is illustrated in the regression plot (**Figure 3b**) too**.** As a result, during the winter season, the lower air temperature contributed to elevated HgP levels due to a higher partitioning coefficient and, hence, more mercury in the particulate phase. The significant negative correlation between HgP and temperature showed that the Hg adsorption onto the particles surface was the main process for HgP formation at these sites.

In addition, during wintertime, particulate matter accumulation, because of decreased planetary boundary layer height and increased particulate matter emission because of enhanced combustion activities for space heating, provided more space for Hg species adsorption onto particles as well as increased oxidation reactions of GEM to produce more HgP, while the possible explanation for lower concentrations of Hg in the particulate phase during summer was the liberation of volatile mercury adsorbed onto particles due to the decrease of the partitioning coefficient at higher atmospheric temperatures.

3.5.2. Influence of relative humidity and precipitation on atmospheric HgP levels

In the atmosphere, gaseous Hg^{2+} and semi-volatile organic compounds behave similarly, and their partitioning onto aerosols is greatly influenced by relative humidity, and they have effective partitioning onto aerosols at high relative humidity [82,83]. In the atmosphere, water droplets or liquid water are likely to form at higher relative humidity. Several studies demonstrated that the aqueous or heterogeneous

reactions in water droplets or liquid water accelerated the transformation of mercury, while the weak acidic environment in liquid droplets facilitated the reactions between gaseous Hg and ions such as SO_4^{2-}, SO_3^{2-}, Cl^-, S^{2-}, HS^-, and H_2O_2 [48,84,85]. Subir et al. [86] also reviewed that GEM was not likely to react with OH or O_3 in the gas phase because of the low reaction constant, but GEM could be transformed to oxidized Hg by rapid oxidation reactions in the aqueous phase. These studies or reviews pointed to the HgP formation pathway through adsorption of gaseous Hg onto particle surfaces followed by aqueous phase oxidation reactions in droplets at high relative humidity [85].

The Pearson correlation coefficient (**Table 4**) between HgP level and relative humidity showed a significantly positive correlation at JNU ($r^2 = 0.151$, $P < 0.05$) and Badarpur ($r^2 = 0.343$, $P < 0.05$), and a significantly negative correlation with relative humidity at Okhla ($r^2 = 0.213$, $P < 0.05$). It is illustrated in the regression plot (**Figure 3c**) too. At JNU and Badarpur, high relative humidity was observed during wintertime sampling, mainly due to very dense fog and static weather conditions, which contributed to HgP accumulation in the atmosphere, mainly due to adsorption of gaseous Hg onto particle surfaces followed by aqueous phase oxidation reactions in fog or liquid droplets [48,87]. At Okhla, monsoon time sampling was carried out during peak rainy season that observed high relative humidity which led to wet deposition or scavenging of HgP through precipitation, and therefore, lower HgP concentrations. While wintertime sampling was carried out in October and November, high HgP concentrations were observed during this period. The low relative humidity as well as clear weather and no foggy conditions were observed during this period; therefore, a negative correlation between HgP and relative humidity was observed at Okhla.

Total suspended particulate matter is most efficiently removed from the atmosphere by precipitation or wet scavenging [88]. Precipitation controls the scavenging rate of HgP and plays a significant role in HgP removal from the atmosphere by processes of wet scavenging or precipitation [10]. Previous studies have also reported a dramatic decrease in the concentrations of HgP after every heavy precipitation event and during monsoon season [48,54,57]. We have also found lower HgP concentrations after precipitation events at both the sites (JNU and Okhla) during monsoon seasons, and higher HgP concentrations without precipitation during monsoon and dry seasons. At Okhla, sampling of the monsoon season was carried out during peak monsoon, which had high relative humidity, and therefore, frequent and high amounts of precipitation were observed, which led to washout of HgP and hence lower HgP concentrations, while at JNU, during monsoon sampling, low humidity and therefore less precipitation were observed. Therefore, the precipitation significantly affected atmospheric HgP concentrations at JNU and Okhla. Since frequent and high amounts of precipitation mainly happened at higher relative humidity during monsoon, therefore, frequent and higher precipitation amounts were also a factor that contributed to lower HgP concentrations during monsoon at Okhla [42]. These findings were also reinforced by a significant negative relationship between relative humidity and HgP at Okhla. Therefore, we can conclude that atmospheric HgP was affected greatly by weather, time of sampling, and source emission intensity.

3.5.3. Influence of wind speed and wind direction on atmospheric HgP levels

In the atmosphere, wind direction and speed play an important role in the dilution and dispersion of air pollutants and their transport from sources to receptors. The higher wind speed dilutes or disperses air pollutants, while calm wind restricts the dilution or dispersion of air pollutants, leading to accumulation and stagnation of air pollutants. In Delhi, especially in the winter season, lower wind speed combined with lower temperature causes temperature inversion conditions, which in turn leads to the accumulation of atmospheric pollutants and deteriorates the air quality.

The Pearson correlation coefficient (**Table 4**) between HgP levels and wind speed showed a significantly positive correlation at JNU (r^2 = 0.143, $P < 0.05$), and a negative correlation with wind speed at Okhla (r^2 = 0.067, P = 0.21) and Badarpur (r^2 = 0.075, P = 0.37), but the correlation was not significant at Okhla and Badarpur. It is illustrated in the regression plot (**Figure 3d**) too**.** At JNU, the significantly positive correlation between wind speed and HgP levels showed a strong influence of wind speed on HgP. Since active sources of Hg were not present in JNU, the significantly positive correlation between wind speed and HgP levels showed that, as compared to the sources inside the JNU, HgP was predominantly transported from other regions via local, regional, and trans-boundary atmospheric transport.

At Okhla and Badarpur, the insignificant correlation between wind speed and HgP levels showed that HgP was not affected much by wind speed, and emissions from anthropogenic sources contributed more to atmospheric HgP. But still, negative correlation showed that higher wind speed led to dispersion and horizontal dilution of atmospheric HgP even after continuous emission from sources, and hence lower HgP, while lower wind speed led to accumulation and less dispersion, and hence higher HgP. Therefore, the negative correlation between wind speed and HgP levels showed that high HgP episodes were observed at relatively low wind speeds, and hence suggested that HgP was predominantly contributed by local emissions from anthropogenic sources. Therefore, at both locations, Okhla and Badarpur, HgP was predominantly contributed by direct emissions from sources as compared to regional transport.

The wind rose and HgP pollution rose at sampling sites (JNU, Okhla, and Badarpur) during the study period is given in **Figure 4**. The wind rose shows the variation of wind speed and wind direction, while the pollution rose shows the variation of HgP concentration with respect to wind speed and wind direction at JNU, Okhla, and Badarpur during the study period.

As shown in **Figure 4**, the prevailing wind direction was W-NW-E at JNU, which accounted for 78% of the whole study period. Generally, the wind speed was high at JNU; 56% was between 8 and 44 km h^{-1}. At JNU, the HgP concentration was always high when the wind speed was high, irrespective of the wind direction. The highest HgP levels were reported when the wind came from the east-south-east direction. This shows that the high wind speed contributed to elevated HgP concentration in JNU irrespective of the wind direction. Therefore, analysis of wind rose and pollution rose and significant positive correlation between wind speed and HgP levels confirmed that, at JNU, HgP was predominantly transported from other regions via local, regional, and trans-boundary atmospheric transport. The prevalent wind direction was

W-NW at Okhla and Badarpur, which accounted for 74% and 77%, respectively, of the whole study period. Generally, the wind speed was low; 89% at Okhla and 54% at Badarpur were under 8 km h^{-1}.

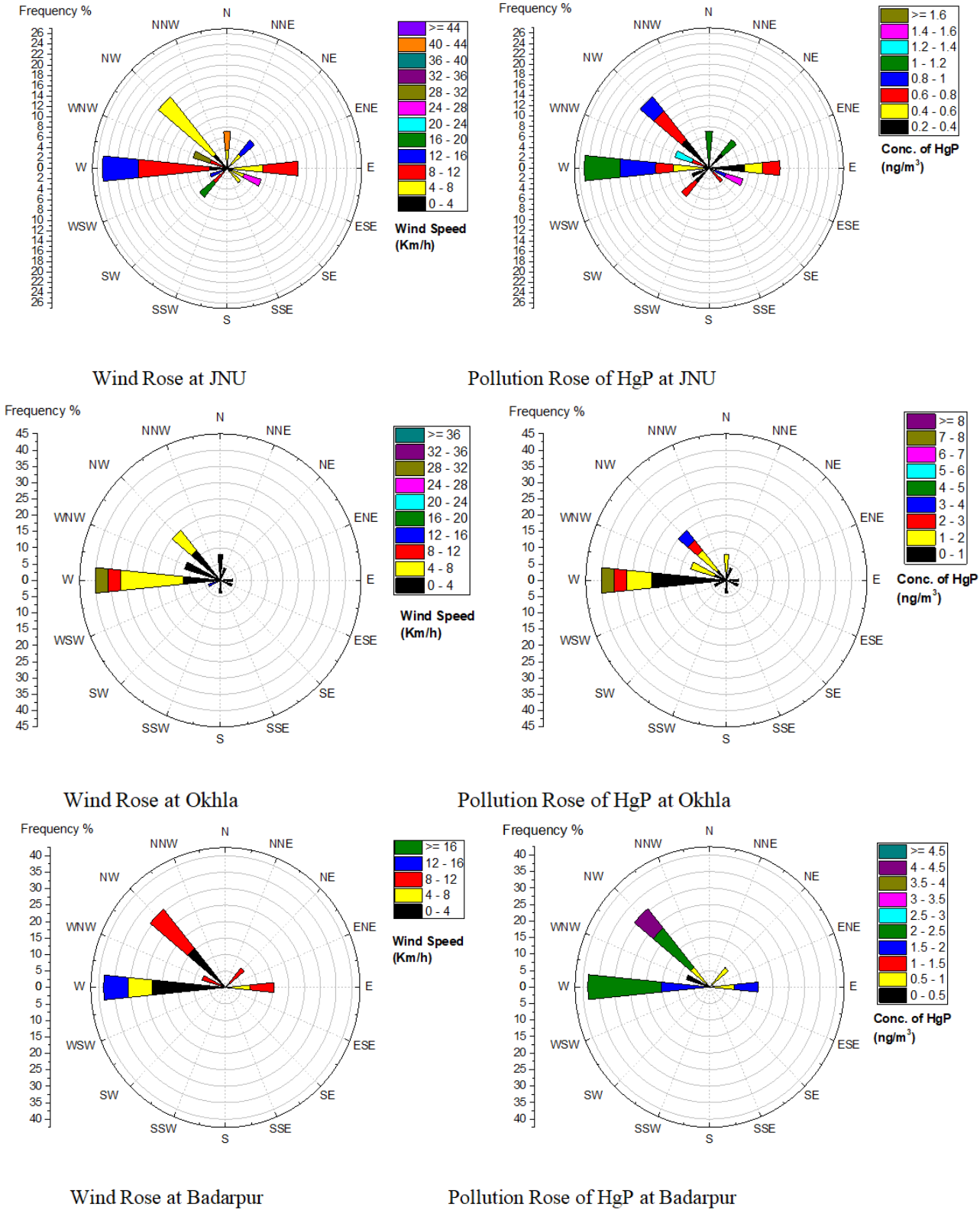

Figure 4. Wind rose and HgP pollution rose at JNU, Okhla, and Badarpur.

As shown in **Figure 4**, at Okhla, the higher HgP levels at lower wind speed were

reported when wind was arriving from the northwest direction. But higher HgP levels at higher wind speeds and lower levels at lower wind speeds were also reported when the wind was arriving from the west direction. It is notable that at Okhla, the HgP concentrations were evidently higher under lower as well as higher wind speeds when the wind was arriving from the northwest and west directions. The highest HgP concentration was reported when the wind came from the west direction. This result indicates that the emissions from nearby sources located very close to the sampling site in the west and northwest directions may be the major contributors to atmospheric HgP at Okhla. The air masses arriving at Okhla from the west and northwest directions were loaded with higher HgP concentrations emitted by the waste incinerator and other industrial activities along the way and brought higher HgP concentrations to the sampling site.

As shown in **Figure 4**, it is notable that at Badarpur, the HgP concentrations were evidently higher under lower as well as higher wind speeds when the wind was arriving from the northwest and west directions. The highest HgP concentration was reported when the wind arrived from the northwest direction. These results showed that the wind blowing from the west and northwest directions always contributed to elevated HgP concentrations at the Badarpur site irrespective of the wind speed. This also indicated that the emissions from nearby sources located very close to the sampling site in the west and northwest directions might be the major contributors to atmospheric HgP at the Badarpur site. The air masses arriving at Badarpur from the west, east, and northwest directions were loaded with higher HgP concentrations emitted by the landfill site, waste incinerator, and other industrial activities along the way and brought higher HgP concentrations to the sampling site. Also, it may be due to winds blowing from the Delhi city area, which is situated in these directions.

Therefore, analysis of pollution rose and wind rose, and an insignificant negative correlation between HgP levels and wind speed reconfirmed that HgP at Okhla and Badarpur was predominantly contributed through nearby local sources, located in the northwest and west directions. At Okhla, the main concern is the waste incinerator plant adjacent to the site in the northwest direction, while at Badarpur, the main concerns are the industries adjacent to the site. As listed in **Figure 1**, a thermal power plant in the east-northeast, and a waste dumping landfill site in the northwest direction are located very close to the Badarpur site, and a waste incinerator plant was also located in the north-northwest direction, but not very close to the site; however, in the west, there were no evident large point sources, and yet there were higher HgP concentrations, which could be contributed by regional transport too. As our sampling sites are located in the urban area, therefore, emissions from traffic, small industrial units, and local residential sources cannot be ignored. In summary, emissions from the coal-fired thermal power plant, traffic, small residential units, waste dumping and landfill, and waste incinerator plants could be the dominant local sources of HgP at these sites, apart from distant sources.

4. Seasonal variation of other trace elements and HgP in ambient air and their sources

Along with HgP, other elements such as Pb, Ni, Zn, Cd, Cr, Fe, Mn, Cr, Cu, Ca,

Mg, K, and Na were also analyzed to find out the possible sources of HgP and its relationship with these elements, as well as to establish the connection of airborne PM_{10} with different sources. The statistical description of concentrations of trace elements in PM_{10} aerosols at JNU, Okhla, and Badarpur during their respective study periods is given in **Table 5**. Pearson's correlation coefficient between HgP and other elements at JNU is given in **Table 6**, and Pearson's correlation coefficient between HgP and other elements at Okhla and Badarpur is given in **Table 7**.

Table 5. Statistical summary for concentrations of other elements in PM_{10} aerosols at JNU, Okhla, and Badarpur.

	Winter			**Monsoon**			**Summer**		
Elements	**Min**	**Max**	**Mean ± SD**	**Min**	**Max**	**Mean ± SD**	**Min**	**Max**	**Mean ± SD**
JNU									
HgP (ng/m^3)	0.32	1.43	0.91 ± 0.37	0.25	0.94	0.53 ± 0.24	0.24	1.18	0.71 ± 0.31
Cu (ng/m^3)	16.9	92.16	41.16 ± 26.7	6.84	38.02	19.07 ± 11.26	25.9	118.8	54.96 ± 31.9
Ni (ng/m^3)	1.92	13.04	6.30 ± 4.16	2.59	11.90	5.03 ± 2.95	3.81	20.09	9.44 ± 5.24
Cr (ng/m^3)	19.3	37.27	31.95 ± 6.61	6.04	84.52	33.21 ± 31.38	17.6	93.68	41.41 ± 23.6
Cd (ng/m^3)	1.65	42.84	9.87 ± 11.8	<DL	1.34	0.28 ± 0.49	0.05	16.60	3.66 ± 5.16
Pb (µg/m^3)	0.14	0.71	0.51 ± 0.20	0.02	0.91	0.27 ± 0.31	0.12	0.36	0.22 ± 0.08
Mn (µg/m^3)	0.04	0.47	0.15 ± 0.14	0.02	0.06	0.04 ± 0.02	0.05	0.22	0.11 ± 0.06
Fe (µg/m^3)	0.28	0.50	0.37 ± 0.08	0.15	0.33	0.25 ± 0.08	0.31	2.09	0.95 ± 0.49
Zn (µg/m^3)	0.22	0.43	0.30 ± 0.08	0.09	0.32	0.16 ± 0.09	0.11	0.97	0.43 ± 0.28
Ca (µg/m^3)	0.33	2.00	0.91 ± 0.62	0.75	2.28	1.24 ± 0.53	0.13	3.11	1.58 ± 1.00
Na (µg/m^3)	0.26	0.92	0.50 ± 0.20	0.27	0.77	0.59 ± 0.18	0.22	0.75	0.49 ± 0.21
Mg (µg/m^3)	2.3*	0.09	0.04 ± 0.03	0.03	0.66	0.15 ± 0.21	0.08	0.47	0.23 ± 0.14
K (µg/m^3)	1.59	3.77	2.41 ± 0.70	0.33	0.72	0.58 ± 0.15	0.74	4.10	2.49 ± 1.28
Okhla									
HgP (ng/m^3)	0.40	7.36	2.33 ± 1.94	0.19	1.73	0.79 ± 0.48			
Cu (ng/m^3)	33.9	191.5	100.8 ± 45.4	16.2	106.9	37.7 ± 25.1			
Ni (ng/m^3)	5.69	23.41	15.6 ± 6.62	3.39	11.33	5.88 ± 2.22			
Cr (ng/m^3)	3.80	66.84	39.4 ± 25.0	9.51	41.40	18.5 ± 7.63			
Cd (ng/m^3)	1.74	23.24	8.55 ± 5.74	0.00	26.66	3.61 ± 6.94			
Pb (µg/m^3)	0.16	0.87	0.47 ± 0.23	0.03	0.19	0.09 ± 0.05			
Mn (µg/m^3)	0.05	0.19	0.12 ± 0.05	0.06	0.38	0.15 ± 0.08			
Fe (µg/m^3)	0.60	1.59	0.94 ± 0.33	0.20	0.88	0.54 ± 0.23			
Zn (µg/m^3)	0.16	0.87	0.56 ± 0.25	0.08	0.50	0.23 ± 0.13			
Ca (µg/m^3)	3.30	8.52	5.62 ± 1.69	0.50	2.70	1.27 ± 0.71			
Na (µg/m^3)	0.61	2.17	1.34 ± 0.51	0.20	1.82	0.74 ± 0.57			
Mg (µg/m^3)	0.05	0.20	0.12 ± 0.05	0.01	0.08	0.04 ± 0.03			
K (µg/m^3)	1.91	8.13	5.06 ± 1.92	0.64	1.38	0.90 ± 0.21			

Table 5. (*Continued*).

	Winter			Monsoon			Summer		
Elements	**Min**	**Max**	**Mean ± SD**	**Min**	**Max**	**Mean ± SD**	**Min**	**Max**	**Mean ± SD**
Badarpur									
HgP (ng/m^3)	0.30	4.03	1.81 ± 0.96						
Cu (ng/m^3)	37.43	88.16	60.95 ± 17.19						
Ni (ng/m^3)	4.77	13.28	9.13 ± 2.90						
Cr (ng/m^3)	56.78	146.66	95.64 ± 26.63						
Cd (ng/m^3)	3.29	44.37	10.88 ± 10.90						
Pb (µg/m^3)	0.14	0.59	0.28 ± 0.12						
Mn (µg/m^3)	0.06	0.14	0.10 ± 0.03						
Fe (µg/m^3)	0.35	1.14	0.70 ± 0.24						
Zn (µg/m^3)	0.25	1.05	0.64 ± 0.22						
Ca (µg/m^3)	4.06	9.33	6.21 ± 1.61						
Na (µg/m^3)	0.55	1.38	0.94 ± 0.28						
Mg (µg/m^3)	0.09	0.34	0.22 ± 0.10						
K (µg/m^3)	0.28	4.07	2.84 ± 1.03						

DL = Detection limit.
* ng/m^3.

Table 6. Pearson's correlation coefficient between HgP concentration and other elements at JNU.

	HgP	**Pb**	**Cu**	**Mn**	**Fe**	**Ni**	**Zn**	**Cr**	**Cd**	**Mg**	**Na**	**K**	**Ca**
JNU Winter													
HgP	1												
Pb	**0.67***	1											
Cu	0.12	0.30	1										
Mn	0.37	0.46	−0.02	1									
Fe	−0.04	0.16	**0.69***	0.14	1								
Ni	0.07	0.36	**0.89****	0.17	**0.61***	1							
Zn	0.11	0.39	**0.94****	0.26	**0.69***	**0.94****	1						
Cr	0.05	−0.27	0.16	**−0.60***	0.27	−0.08	−0.05	1					
Cd	−0.1	0.31	**0.84****	−0.05	**0.62***	**0.75****	**0.80****	0.16	1				
Mg	−0.50	**−0.67***	0.43	−0.60	0.22	0.22	0.25	0.39	0.33	1			
Na	0.03	0.17	**0.81****	−0.36	0.29	**0.68***	**0.67***	0.38	**0.78****	0.48	1		
K	0.00	−0.03	**0.90****	−0.23	**0.62***	**0.78****	**0.79****	0.31	0.60	**0.65***	**0.73***	1	
Ca	−0.37	−0.51	0.52	−0.49	0.35	0.31	0.33	0.34	0.55	**0.90****	0.51	**0.63***	1
JNU Monsoon													
HgP	1												
Pb	−0.48	1											
Cu	0.22	0.21	1										
Mn	0.08	−0.22	0.37	1									
Fe	−0.18	0.05	0.52	**0.88****	1								
Ni	0.63	−0.04	0.60	0.61	0.46	1							

Table 6. (*Continued*).

	HgP	Pb	Cu	Mn	Fe	Ni	Zn	Cr	Cd	Mg	Na	K	Ca
JNU Monsoon													
Zn	0.18	−0.08	0.48	0.60	0.41	0.38	1						
Cr	0.34	−0.36	0.22	**0.77***	0.41	0.61	**0.74***	1					
Cd	0.14	0.12	0.29	0.06	0.02	−0.01	**0.73***	0.15	1				
Mg	0.63	−0.20	0.43	0.60	0.42	**0.96****	0.18	0.58	−0.26	1			
Na	**0.76***	−0.36	−0.22	−0.23	−0.38	0.34	−0.35	−0.11	−0.13	0.43	1		
K	−0.24	0.59	0.65	0.52	**0.77***	0.39	0.41	0.08	0.36	0.21	−0.37	1	
Ca	−0.45	0.39	−0.01	0.05	0.44	−0.18	−0.39	−0.57	−0.11	−0.17	−0.06	0.56	1
JNU Summer													
HgP	1												
Pb	−0.16	1											
Cu	0.53	0.44	1										
Mn	0.66	0.28	0.44	1									
Fe	0.57	0.30	0.43	**0.76***	1								
Ni	0.65	0.49	**0.71***	**0.85****	**0.90****	1							
Zn	0.37	0.10	**0.75***	0.43	0.29	0.47	1						
Cr	0.59	−0.03	0.36	0.32	**0.72***	0.59	−0.03	1					
Cd	0.14	0.30	**0.77***	0.02	−0.23	0.16	0.66	−0.21	1				
Mg	0.59	0.31	0.36	**0.98****	**0.74***	**0.81****	0.42	0.21	−0.04	1			
Na	0.38	0.35	0.20	**0.80****	**0.78***	**0.72***	0.35	0.16	−0.2	**0.90****	1		
K	0.26	0.55	0.41	**0.73***	0.53	**0.67***	0.52	−0.13	0.21	**0.81****	**0.85****	1	
Ca	0.28	0.35	0.23	**0.83****	0.48	0.57	0.49	−0.19	0.03	**0.90****	**0.83****	**0.82****	1

*. Correlation is significant at the 0.05 level (2-tailed).
**. Correlation is significant at the 0.01 level (2-tailed).

Table 7. Pearson's correlation coefficient between HgP concentration and other elements at Okhla and Badarpur.

	HgP	Pb	Cu	Mn	Fe	Ni	Zn	Cr	Cd	Mg	Na	K	Ca
Okhla Winter													
HgP	1												
Pb	0.10	1											
Cu	−0.07	0.60	1										
Mn	−0.10	0.51	0.49	1									
Fe	−0.18	0.47	0.44	**0.97****	1								
Ni	−0.2	0.53	**0.65***	**0.89****	**0.82****	1							
Zn	−0.21	0.43	**0.71***	**0.86****	**0.82****	**0.91****	1						
Cr	−0.13	0.20	0.18	**0.78****	**0.75***	0.62	**0.73***	1					
Cd	0.05	0.49	**0.80****	0.07	0.06	0.32	0.28	−0.34	1				
Mg	−0.1	0.52	0.38	**0.98****	**0.94****	**0.81****	**0.76***	**0.78****	−0.06	1			
Na	0.02	**0.64***	0.51	**0.97****	**0.89****	**0.88****	**0.78****	**0.69***	0.11	**0.97****	1		
K	0.15	**0.74***	**0.69***	**0.88****	**0.78****	**0.84****	**0.79****	0.61	0.30	**0.86****	**0.95****	1	

Table 7. (*Continued*).

	HgP	Pb	Cu	Mn	Fe	Ni	Zn	Cr	Cd	Mg	Na	K	Ca
Okhla Winter													
HgP	1												
Ca	−0.11	**0.73***	**0.65***	**0.83****	**0.75***	**0.72***	**0.69***	0.49	0.29	**0.84****	**0.88****	**0.90****	1
Okhla Monsoon													
HgP	1												
Pb	0.3	1											
Cu	−0.24	**0.72****	1										
Mn	−0.02	−0.01	−0.31	1									
Fe	−0.26	0.14	0.47	−0.45	1								
Ni	−0.4	0.46	**0.73****	−0.44	0.31	1							
Zn	0.16	**0.85****	**0.65****	−0.21	0.07	**0.63***	1						
Cr	0.44	**0.54***	0.10	−0.17	−0.09	0.06	0.46	1					
Cd	−0.10	**0.71****	**0.90****	−0.18	0.17	**0.61***	**0.56***	0.2	1				
Mg	−0.27	−0.07	0.38	−0.40	**0.86****	0.21	−0.13	−0.41	0.17	1			
Na	−0.25	−0.27	0.13	−0.33	**0.73****	0.05	−0.27	−0.48	−0.09	**0.91****	1		
K	0.27	**0.54***	**0.52***	−0.49	**0.69****	0.19	0.40	0.40	0.36	0.49	0.26	1	
Ca	−0.14	0.07	0.35	−0.23	**0.54***	0.18	0.11	−0.43	0.21	**0.81****	**0.76****	0.36	1
Badarpur Winter													
HgP	1												
Pb	**0.66***	1											
Cu	0.17	**0.70****	1										
Mn	0.08	**0.64***	**0.87****	1									
Fe	0.30	**0.80****	**0.82****	**0.90****	1								
Ni	0.12	**0.68***	**0.67***	0.55	**0.68***	1							
Zn	0.31	0.55	0.47	0.50	0.46	0.52	1						
Cr	0.24	−0.06	−0.39	−0.28	−0.19	−0.51	0.02	1					
Cd	0.15	−0.01	−0.14	0.11	0.12	−0.48	0.05	**0.71****	1				
Mg	−0.04	0.37	0.42	0.36	0.55	**0.86****	0.32	−0.43	−0.39	1			
Na	0.18	0.54	0.44	0.51	**0.64***	**0.86****	**0.56***	−0.41	−0.32	**0.87****	1		
K	0.04	−0.12	−0.15	−0.04	0.01	0.19	−0.05	−0.38	−0.14	0.51	0.44	1	
Ca	0.38	**0.70****	0.51	**0.60***	**0.72****	**0.79****	**0.59***	−0.26	−0.13	**0.73****	**0.93****	0.34	1

*. Correlation is significant at the 0.05 level (2-tailed).
**. Correlation is significant at the 0.01 level (2-tailed).

At JNU, the highest average values of Mg, Ca, and K in summers, and higher average values of Ca and Mg in monsoons, suggested a greater influence of crustal contributions resulting from heavy dust storms, a common phenomenon during these seasons [89], which suggested some loading of HgP to the atmosphere along with the crustal components. The average values of HgP and crustal components suggest less crustal and more anthropogenic contribution to HgP during winters, which was also supported by the correlation study, as shown in **Table 6**. The highest average values

of Na during monsoon season indicated its contribution from crustal as well as sea salts/marine aerosols [90], which suggested a higher influence of marine aerosols on HgP, which was also supported by a significant positive correlation of Na with HgP in monsoon season, as shown in **Table 6**. The higher concentration of K during summer and winter shows a greater influence of biomass burning, as K is broadly known as a tracer of biomass burning emissions [91], and therefore, burning of biomass also contributed to atmospheric HgP [92], especially in winter and summer samples. The highest concentration of HgP, Pb, Mn, and Cd during the winter season indicates industrial as well as vehicular contribution of these metals [93,94]. The lower concentrations of atmospheric HgP and these metals during monsoon could be due to the scavenging effect of rain events. The highest concentration of Ni, Zn, Cu, Fe, Cr, Ca, Mg, and K during summer indicates their contribution through re-suspension of soil and road dust through wind and vehicles [95].

At JNU, during the winter season, a significant to moderate positive correlation of Cu, Fe, Ni, Zn, Cr, and Cd with each other, and with other metals such as Ca, Mg, K, and Na (**Table 6**) suggested both crustal and anthropogenic contributions of PM_{10} aerosols, most possibly through re-suspension of soil/road dust mixed with previously emitted metals from vehicles in the form of exhaust and brake wear, and emissions from industries [88,96]. The negative correlation of HgP, Pb, and Mn with crustal elements suggested that these were not contributed by crustal components, while the stronger positive correlation between HgP and Pb, and the moderate positive correlation between HgP and Mn, suggested their common sources, most probably from industries or anthropogenic sources.

At JNU, during the summer season, the stronger positive correlation of Ca, Mg, K, and Na with each other, and the slightly to stronger positive correlation of these crustal elements with other elements except Cr and Cd (**Table 6**), suggested the contribution of PM_{10} aerosols from both crustal and anthropogenic sources [88,96]. The slightly positive correlation of HgP with Ca, K, Na, Zn, and Cd, and the moderate positive correlation of HgP with Cu, Mn, Fe, Ni, Cr, and Mg, observed during the summer season, suggested the contribution of atmospheric HgP from both crustal and anthropogenic sources.

At JNU, during the monsoon season, crustal elements were not significantly correlated with each other, as well as most of the other elements (**Table 6**). There was a slightly positive correlation between Ca and K and between Mg and Na only. This suggested less crustal contribution to PM_{10} aerosols, most probably due to washout of particulate matter, as well as crustal elements through wet scavenging during rain events. The correlations between other elements were also not significant except for a few such as HgP with Na, Mn with Fe and Cr, Fe with K, Ni with Mg, and Zn with Cr and Cd. A strong positive correlation of HgP with Na observed during the monsoon season suggested a higher influence of marine aerosols [90].

At Okhla, the average values of other elements in the atmosphere had more pronounced seasonality. The average values of all the elements except Mn were highest during the winter season at Okhla. The average value of atmospheric HgP was the lowest as compared to other elements during both seasons. However, the highest concentrations of HgP and other elements except Mn during winter, suggested a higher influence of emissions from industrial, vehicular, and anthropogenic sources

[93,94,96], and less dispersion due to the lowering of atmospheric boundary layer height during winters. Another possible reason for high concentrations of HgP and other elements during winters might be the MSW and medical waste incineration [94], as an incinerator-based waste-to-energy plant was located near the residential colony where the sampling was carried out. The exhaust gases coming from the waste incineration plant may contain many potentially toxic and harmful heavy metals along with other pollutants [94]. The lower concentrations of all these elements, during monsoon, could be due to the scavenging effect of rain events (wet deposition), as some light to heavy rainfall events were observed during monsoon sampling.

At Okhla, the HgP was not correlated with other elements during the winter season (**Table 7**). Therefore, no inferences could be concluded by the correlation study for the sources of mercury during the winter season. Hence, mercury might have been contributed by unique independent sources, most probably the dumping of Hg-containing discarded items like CFLs, fluorescent tubes, thermometers, thermostats, batteries, and other products in the MSW dumping and landfill site, as well as the incineration of Hg-containing MSW and medical waste in incinerator plants [94], which are located nearby the sampling site. During the monsoon season, there was no strong correlation between HgP and other elements; only a slight to moderate positive correlation of HgP with Pb and Cr was observed, suggesting the influence of anthropogenic sources. The negative correlation of HgP with Ca, Na, and Mg shows that HgP was not contributed by crustal components during the monsoon season.

At Badarpur, the concentrations of other elements were measured during the winter season only. When the mean values of other elements at Badarpur were compared to the mean values of other elements at Okhla and JNU, the highest mean values of Zn, Cr, Cd, and Ca, and the second-highest mean values of HgP, Cu, Mg, and K were observed at Badarpur, suggesting both anthropogenic and natural sources contributed to the atmospheric particulate matter at Badarpur. One of the NTPC's TPP was located near the residential colony where sampling was carried out. Metals are present in the coal as a natural contaminant. During the coal combustion process in coal-fired TPPs, trace metals in coal are released into the atmosphere. At Badarpur, the significant positive correlation of HgP with Pb, and the slightly positive correlation of HgP with Fe, Zn, and Ca (**Table 7**) were observed during the winter season, suggesting the contribution of atmospheric HgP from both crustal and anthropogenic sources. Also, HgP emissions from MSW dumping and landfill sites, as well as MSW and medical waste incineration [94], cannot be ruled out because these sources were not very far from the sampling site.

5. Air trajectory analysis

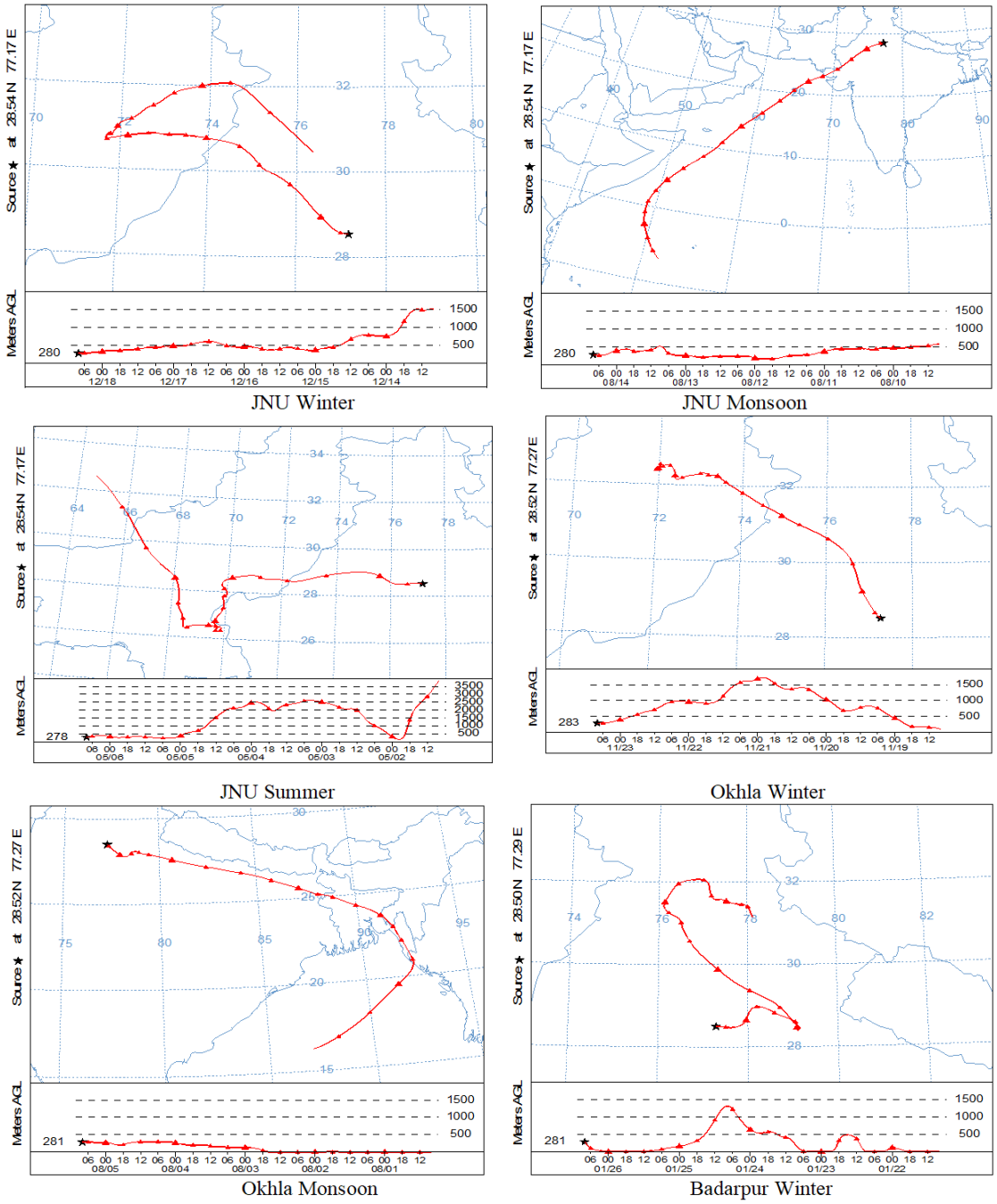

Figure 5. Representative air trajectories reaching at the JNU, Okhla, and Badarpur sites.

To understand the probable local/distant sources, the origin of the air parcel was backtracked using the National Oceanic and Atmospheric Administration (NOAA) HYSPLIT model with an input of GDAS Meteorological Data at an atmospheric height of 500 m above mean sea level [97,98]. Five-day air mass backward trajectories were calculated for each sampling day at all sampling sites; the representative trajectories at each site are given in **Figure 5**. Backward trajectories from HYSPLIT showed that the HgP and other elements were derived from regional air masses and marine and local anthropogenic emission sources. During monsoon season, there are

two sources of origin of air masses coming to the Indian subcontinent. One type of air mass originates from the Indian Ocean and then travels a long way from the Arabian Sea and western parts of India; the other type of air mass originates from the Indian Ocean and then travels a long way from the Bay of Bengal and eastern parts of India. At JNU, during monsoon, most of the air masses originated from the Arabian Sea and retained their marine characteristics, which was reflected by the significant positive correlation between Na and HgP (**Table 6**), and the highest average concentration of Na during monsoon as compared to winter and summer seasons (**Table 5**). At Okhla, during monsoon, most of the air masses originated from the Bay of Bengal and carried anthropogenic emissions while traveling a long way from the eastern parts of India and lost their marine identity, which was reflected by the negative correlation between Na and HgP (**Table 7**), and lower average concentration of Na during monsoon as compared to the winter season (**Table 5**). During the winter season at all three sites and during the summer season at JNU, most of the time inland-originated air masses travelled to the sampling sites, and they carried pollution from local anthropogenic sources, as already explained in the previous sections. Interestingly, even though the distance between these sites is not huge, air masses are traveling to the sampling sites from two majorly different directions during monsoon season.

6. Conclusion

This study presents the first-ever measurements of particulate mercury (HgP) concentration at three sites in Delhi, i.e., JNU, Okhla, and Badarpur. The average concentrations of HgP were 0.74 ± 0.35 ng m^{-3}, 1.40 ± 1.46 ng m^{-3}, and 1.81 ± 0.96 ng m^{-3} at JNU, Okhla, and Badarpur, respectively, during their respective study periods. The average concentrations of HgP were observed to be higher during the winters as compared to summer and monsoon seasons at all the sites because of the influence of variations in the intensity of direct Hg emissions from anthropogenic point sources, gas-particle partition of mercury species, as well as other influencing meteorological factors, i.e., humidity, precipitation, wind speed and directions, and ambient temperature. The wind and pollution studies showed that the sampling sites were affected by local, regional, and transboundary pollution sources, with JNU having more influence from regional and transboundary pollution sources, while Okhla and Badarpur had more influence from local sources. Trajectory analysis showed that air masses traveling to the JNU site from the Arabian Sea during monsoon season retained their marine characteristics, which was also supported by the correlation study. While air masses traveling to Okhla from the Bay of Bengal during monsoon lost their marine characteristics, which was also supported by the correlation study. The global comparison shows that the HgP levels in Delhi were significantly higher than most cities in Europe and North America, and were approximately comparable to the values reported from most sites in Asia, and were less compared to the values reported from other studies in India. The harmful effects of Hg on human health are widely discussed in the literature. However, it is difficult to assess the harmfulness of these levels of HgP, because there is no standard value available as a National Ambient Air Quality Standard (NAAQS). Therefore, it could be appropriate to include Hg in NAAQS, so that regular monitoring of Hg, like other criteria

pollutants, can be carried out. This study serves as an important baseline for HgP levels in Delhi, and will also serve as an important reference for future assessment of HgP pollution in Delhi. Anthropogenic HgP in the capital city of India still needs further long-term monitoring programs because of growing urbanization and industrialization.

Author contributions: Conceptualization, UCK; methodology, UCK and AK; software, AK; validation, UCK and AK; formal analysis, AK; investigation, AK; resources, UCK and AK; data curation, AK and UCK; writing—original draft preparation, AK; writing—review and editing, UCK; visualization, UCK and AK; supervision, UCK; project administration, UCK; funding acquisition, AK and UCK. All authors have read and agreed to the published version of the manuscript.

Acknowledgments: The present work was supported by financial assistance received from JNU as UGC-UPA II project (UCK) and DST-PURSE grants (UCK). Anita Kumari sincerely acknowledges the Fellowship (Shyama Prasad Mukherjee Fellowship award) from CSIR, India.

Institutional review board statement: Not applicable.

Informed consent statement: Not applicable.

Conflict of interest: The authors declare no conflict of interest.

References

1. Basu N, Bastiansz A, Dórea JG, et al. Our evolved understanding of the human health risks of mercury. Ambio. 2023; 52(5): 877-896. doi: 10.1007/s13280-023-01831-6
2. Weiss-Penzias PS, Bank MS, Clifford DL, et al. Marine fog inputs appear to increase methylmercury bioaccumulation in a coastal terrestrial food web. Scientific Reports. 2019; 9(1). doi: 10.1038/s41598-019-54056-7
3. López-Berenguer G, Peñalver J, Martínez-López E. A critical review about neurotoxic effects in marine mammals of mercury and other trace elements. Chemosphere. 2020; 246: 125688. doi: 10.1016/j.chemosphere.2019.125688
4. Obrist D, Kirk JL, Zhang L, et al. A review of global environmental mercury processes in response to human and natural perturbations: Changes of emissions, climate, and land use. Ambio. 2018; 47(2): 116-140. doi: 10.1007/s13280-017-1004-9
5. Li ML, Kwon SY, Poulin BA, et al. Internal Dynamics and Metabolism of Mercury in Biota: A Review of Insights from Mercury Stable Isotopes. Environmental Science & Technology. 2022; 56(13): 9182-9195. doi: 10.1021/acs.est.1c08631
6. Schiavo B, Morton-Bermea O, Salgado-Martínez E, et al. Health risk assessment of gaseous elemental mercury (GEM) in Mexico City. Environmental Monitoring and Assessment. 2022; 194(7). doi: 10.1007/s10661-022-10107-7
7. Padalkar PP, Chakraborty P, Chatterjee S, et al. Mercury speciation in a complex tropical estuarine system: Understanding natural and anthropogenic influences. Regional Studies in Marine Science. 2025; 82: 104000. doi: 10.1016/j.rsma.2024.104000
8. Pacyna JM, Travnikov O, De Simone F, et al. Current and future levels of mercury atmospheric pollution on a global scale. Atmospheric Chemistry and Physics. 2016; 16(19): 12495-12511. doi: 10.5194/acp-16-12495-2016
9. Lin CJ, Pehkonen SO. The chemistry of atmospheric mercury: a review. Atmospheric Environment. 1999; 33(98): 2067-2079.
10. Schroeder WH, Munthe J. Atmospheric mercury - an overview. Atmospheric Environment. 1998; 32(5): 809–822.
11. Shannon JD, Voldner EC. Modeling atmospheric concentrations of mercury and deposition to the Great Lakes. Atmospheric Environment. 1995; 29: 1649–1661.
12. Moore CW, Obrist D, Luria M. Atmospheric mercury depletion events at the Dead Sea: Spatial and temporal aspects. Atmospheric Environment. 2013; 69: 231-239. doi: 10.1016/j.atmosenv.2012.12.020
13. Fang F, Wang Q, Li J. Atmospheric particulate mercury concentration and its dry deposition flux in Changchun City, China.

Science of The Total Environment. 2001; 281: 229–236.
14. Lu J, Schroeder W. Sampling and determination of particulate mercury in ambient air: a review. Water, Air, & Soil Pollution. 1999; 112: 279–295.
15. Schleicher NJ, Schäfer J, Blanc G, et al. Atmospheric particulate mercury in the megacity Beijing: Spatio-temporal variations and source apportionment. Atmospheric Environment. 2015; 109: 251-261. doi: 10.1016/j.atmosenv.2015.03.018
16. Mohan M, Bhati S, Gunwani P, et al. Emission Inventory of Air Pollutants and Trend Analysis Based on Various Regulatory Measures Over Megacity Delhi. Air Quality - New Perspective. Published online July 26, 2012. doi: 10.5772/45874
17. Garg A, Shukla PR, Kapshe M. The sectoral trends of multigas emissions inventory of India. Atmospheric Environment. 2006; 40(24): 4608-4620. doi: 10.1016/j.atmosenv.2006.03.045
18. Karunasagar D, Balarama Krishna MV, Anjaneyulu Y, et al. Studies of mercury pollution in a lake due to a thermometer factory situated in a tourist resort: Kodaikkanal, India. Environmental Pollution. 2006; 143(1): 153-158. doi: 10.1016/j.envpol.2005.10.032
19. Balarama Krishna MV, Karunasagar D, Arunachalam J. Study of mercury pollution near a thermometer factory using lichens and mosses. Environmental Pollution. 2003; 124(3): 357-360.
20. Jayasekher T. Aerosols near by a coal fired thermal power plant: Chemical composition and toxic evaluation. Chemosphere. 2009; 75(11): 1525-1530. doi: 10.1016/j.chemosphere.2009.02.001
21. Pervez S, Koshle A, Pervez Y. Study of spatiotemporal variation of atmospheric mercury and its human exposure around an integrated steel plant, India. Atmospheric Chemistry and Physics. 2010; 10(12): 5535-5549. doi: 10.5194/acp-10-5535-2010
22. Kumari A, Kumar B, Manzoor S, et al. Status of Atmospheric Mercury Research in South Asia: A Review. Aerosol and Air Quality Research. 2015; 15(3): 1092-1109. doi: 10.4209/aaqr.2014.05.0098
23. Morton-Bermea O, Garza-Galindo R, Hernández-Álvarez E, et al. Atmospheric PM2.5 Mercury in the Metropolitan Area of Mexico City. Bulletin of Environmental Contamination and Toxicology. 2018; 100(4): 588-592. doi: 10.1007/s00128-018-2288-6
24. Kumari A, Kulshrestha U. Trace ambient levels of particulate mercury and its sources at a rural site near Delhi. Journal of Atmospheric Chemistry. 2018; 75(4): 335-355. doi: 10.1007/s10874-018-9377-0
25. Li Y, Wang Y, Li Y, et al. Characteristics and potential sources of atmospheric particulate mercury in Jinan, China. Science of The Total Environment. 2017; 574: 1424-1431. doi: 10.1016/j.scitotenv.2016.08.069
26. Kulshrestha UC, Nageswara Rao T, Azhaguvel S, et al. Emissions and accumulation of metals in the atmosphere due to crackers and sparkles during Diwali festival in India. Atmospheric Environment. 2004; 38(27): 4421-4425. doi: 10.1016/j.atmosenv.2004.05.044
27. Bonfil Y, Brand M, Kirowa-Eisner E. Trace determination of mercury by Anodic Stripping Voltammetry at the rotating gold electrode. Analytica Chimica Acta. 2000; 424(1): 65-76.
28. Nguyen TTK, Luu HT, Vu LD, et al. Determination of Total Mercury in Solid Samples by Anodic Stripping Voltammetry. Singh AK, ed. Journal of Chemistry. 2021; 2021: 1-8. doi: 10.1155/2021/8888879
29. Planková A, Jampílek J, Švorc Ľ, et al. Anodic Stripping Voltammetry: affordable and reliable alternative to inductively coupled plasma-based analytical methods. Monatshefte für Chemie - Chemical Monthly. 2018; 149(5): 913-920. doi: 10.1007/s00706-017-2138-y
30. Farghaly OA, Ghandour MA. Square-wave stripping voltammetry for direct determination of eight heavy metals in soil and indoor-airborne particulate matter. Environmental Research. 2005; 97(3): 229-235. doi: 10.1016/j.envres.2004.07.007
31. Nedeltcheva T, Atanassova M, Dimitrov J, et al. Determination of mobile form contents of Zn, Cd, Pb and Cu in soil extracts by combined stripping voltammetry. Analytica Chimica Acta. 2005; 528(2): 143-146. doi: 10.1016/j.aca.2004.10.036
32. Harikumar PS, Dhruvan A, Sabna V, Babitha A. Study on the leaching of mercury from compact fluorescent lamps using stripping voltammetry. Journal of Toxicology and Environmental Health Sciences. 2011; 3(1): 008-013.
33. Arora A, Kumari A, Kulshrestha U. Respirable Mercury Particulates and Other Chemical Constituents in Festival Aerosols in Delhi. Current World Environment. 2018; 13(1): 03-14. doi: 10.12944/cwe.13.1.02
34. Metrohm. Determination of mercury at the rotating gold electrode by Anodic Stripping Voltammetry. Available online: https://www.metrohm.com/content/dam/metrohm/shared/documents/application-bulletins/AB-096_5.pdf (accessed on 23 July 2018).
35. Fu X, Liu C, Zhang H, et al. Isotopic compositions of atmospheric total gaseous mercury in 10 Chinese cities and implications for land surface emissions. Atmospheric Chemistry and Physics. 2021; 21(9): 6721-6734. doi: 10.5194/acp-21-

6721-2021
36. Sakata M, Marumoto K. Formation of atmospheric particulate mercury in the Tokyo metropolitan area. Atmospheric Environment. 2002; 36: 239–246.
37. Gabriel MC, Williamson DG, Brooks S. Lindberg S. Atmospheric speciation of mercury in two contrasting Southeastern US airsheds. Atmospheric Environment. 2005; 39(27): 4947-4958. doi: 10.1016/j.atmosenv.2005.05.003
38. Rutter AP, Schauer JJ. The effect of temperature on the gas–particle partitioning of reactive mercury in atmospheric aerosols. Atmospheric Environment. 2007; 41(38): 8647-8657. doi: 10.1016/j.atmosenv.2007.07.024
39. Gaspar JA, Widmer NC, Cole JA, Seeker WR. Study of mercury speciation in a simulated municipal waste incinerator flue gas. In: Proceedings of the International Conference on Incineration and Thermal Treatment Technologies; 12-16 May 1997; San Francisco, CA, USA.
40. Chambers A, Knecht M, Soelberg N, et al. Mercury Emissions Control Technologies for Mixed Waste Thermal Treatment. In: Proceedings of the International Conference on Incineration and Thermal Treatment Technologies; 11-15 May 1998; Salt Lake City, Utah, USA.
41. Huang J, Kang S, Guo J, et al. Atmospheric particulate mercury in Lhasa city, Tibetan Plateau. Atmospheric Environment. 2016; 142: 433-441. doi: 10.1016/j.atmosenv.2016.08.021
42. Guo J, Kang S, Huang J, et al. Characterizations of atmospheric particulate-bound mercury in the Kathmandu Valley of Nepal, South Asia. Science of The Total Environment. 2017; 579: 1240-1248. doi: 10.1016/j.scitotenv.2016.11.110
43. Guttikunda SK, Goel R. Health impacts of particulate pollution in a megacity—Delhi, India. Environmental Development. 2013; 6: 8-20. doi: 10.1016/j.envdev.2012.12.002
44. Fang F, Wang Q, Li J. Urban environmental mercury in Changchun, a metropolitan city in Northeastern China: source, cycle, and fate. Science of The Total Environment. 2004; 330(1-3): 159-170. doi: 10.1016/j.scitotenv.2004.04.006
45. Zhang F, Xu L, Chen J, et al. Chemical compositions and extinction coefficients of PM2.5 in peri-urban of Xiamen, China, during June 2009–May 2010. Atmospheric Research. 2012; 106: 150-158. doi: 10.1016/j.atmosres.2011.12.005
46. Jayasekhar T, Kumaresan S, Radhika SL, et al. Statistical Analysis of the Aerosol Elemental Composition in an Industrial Belt. Bulletin of Environmental Contamination and Toxicology. 2004; 73(1). doi: 10.1007/s00128-004-0392-2
47. Guo J, Tripathee L, Kang S, et al. Atmospheric particle-bound mercury in the northern Indo-Gangetic Plain region: Insights into sources from mercury isotope analysis and influencing factors. Geoscience Frontiers. 2022; 13(1): 101274. doi: 10.1016/j.gsf.2021.101274
48. Xiu G, Cai J, Zhang W, et al. Speciated mercury in size-fractionated particles in Shanghai ambient air. Atmospheric Environment. 2009; 43(19): 3145-3154. doi: 10.1016/j.atmosenv.2008.07.044
49. Wang Z, Zhang X, Chen Z, et al. Mercury concentrations in size-fractionated airborne particles at urban and suburban sites in Beijing, China. Atmospheric Environment. 2006; 40(12): 2194-2201. doi: 10.1016/j.atmosenv.2005.12.003
50. Lin H, Tong Y, Yu C, et al. First observation of mercury species on an important water vapor channel in the southeastern Tibetan Plateau. Atmospheric Chemistry and Physics. 2022; 22(4): 2651-2668. doi: 10.5194/acp-22-2651-2022
51. Hu Q, Kang H, Li Z, et al. Characterization of atmospheric mercury at a suburban site of central China from wintertime to springtime. Atmospheric Pollution Research. 2014; 5(4): 769-778. doi: 10.5094/apr.2014.086
52. Xu L, Chen J, Yang L, et al. Characteristics and sources of atmospheric mercury speciation in a coastal city, Xiamen, China. Chemosphere. 2015; 119: 530-539. doi: 10.1016/j.chemosphere.2014.07.024
53. Lin H, Tong Y, Chen L, et al. Unexpectedly high concentrations of atmospheric mercury species in Lhasa, the largest city in the Tibetan Plateau. Atmospheric Chemistry and Physics. 2023; 23(7): 3937-3953. doi: 10.5194/acp-23-3937-2023
54. Zhu J, Wang T, Talbot R, et al. Characteristics of atmospheric mercury deposition and size-fractionated particulate mercury in urban Nanjing, China. Atmospheric Chemistry and Physics. 2014; 14(5): 2233-2244. doi: 10.5194/acp-14-2233-2014
55. Duan L, Cheng N, Xiu G, et al. Characteristics and source appointment of atmospheric particulate mercury over East China Sea: Implication on the deposition of atmospheric particulate mercury in marine environment. Environmental Pollution. 2017; 224: 26-34. doi: 10.1016/j.envpol.2016.10.103
56. Kim SH, Han YJ, Holsen TM, et al. Characteristics of atmospheric speciated mercury concentrations (TGM, Hg(II) and Hg(p)) in Seoul, Korea. Atmospheric Environment. 2009; 43(20): 3267-3274. doi: 10.1016/j.atmosenv.2009.02.038
57. Kim PR, Han YJ, Holsen TM, et al. Atmospheric particulate mercury: Concentrations and size distributions. Atmospheric Environment. 2012; 61: 94-102. doi: 10.1016/j.atmosenv.2012.07.014
58. Nguyen DL, Kim JY, Shim SG, et al. Shipboard and ground measurements of atmospheric particulate mercury and total

mercury in precipitation over the Yellow Sea region. Environmental Pollution. 2016; 219: 262-274. doi: 10.1016/j.envpol.2016.10.020
59. Han YJ, Kim JE, Kim PR, et al. General trends of atmospheric mercury concentrations in urban and rural areas in Korea and characteristics of high-concentration events. Atmospheric Environment. 2014; 94: 754-764. doi: 10.1016/j.atmosenv.2014.06.002
60. Chand D, Jaffe D, Prestbo E, et al. Reactive and particulate mercury in the Asian marine boundary layer. Atmospheric Environment. 2008; 42(34): 7988-7996. doi: 10.1016/j.atmosenv.2008.06.048
61. Pyta H, Rosik-Dulewska C, Czaplicka M. Speciation of Ambient Mercury in the Upper Silesia Region, Poland. Water, Air, and Soil Pollution. 2008; 197(1-4): 233-240. doi: 10.1007/s11270-008-9806-9
62. Pyta H, Rogula-Kozłowska W. Determination of mercury in size-segregated ambient particulate matter using CVAAS. Microchemical Journal. 2016; 124: 76-81. doi: 10.1016/j.microc.2015.08.001
63. Zielonka U, Hlawiczka S, Fudala J, et al. Seasonal mercury concentrations measured in rural air in Southern PolandContribution from local and regional coal combustion. Atmospheric Environment. 2005; 39(39): 7580-7586. doi: 10.1016/j.atmosenv.2005.08.003
64. Li J, Sommar J, Wangberg I, et al. Short-time variation of mercury speciation in the urban of Göteborg during GÖTE-2005. Atmospheric Environment. 2008; 42(36): 8382-8388. doi: 10.1016/j.atmosenv.2008.08.007
65. Weigelt A, Temme C, Bieber E, et al. Measurements of atmospheric mercury species at a German rural background site from 2009 to 2011 – methods and results. Environmental Chemistry. 2013; 10(2): 102. doi: 10.1071/en12107
66. Cheng I, Zhang L, Blanchard P, et al. Concentration-weighted trajectory approach to identifying potential sources of speciated atmospheric mercury at an urban coastal site in Nova Scotia, Canada. Atmospheric Chemistry and Physics. 2013; 13(12): 6031-6048. doi: 10.5194/acp-13-6031-2013
67. Song X, Cheng I, Lu J. Annual atmospheric mercury species in Downtown Toronto, Canada. Journal of Environmental Monitoring. 2009; 11(3): 660. doi: 10.1039/b815435j
68. Rutter AP, Snyder DC, Stone EA, et al. In situ measurements of speciated atmospheric mercury and the identification of source regions in the Mexico City Metropolitan Area. Atmospheric Chemistry and Physics. 2009; 9(1): 207-220. doi: 10.5194/acp-9-207-2009
69. Jiang Y, Cizdziel JV, Lu D. Temporal patterns of atmospheric mercury species in northern Mississippi during 2011–2012: Influence of sudden population swings. Chemosphere. 2013; 93(9): 1694-1700. doi: 10.1016/j.chemosphere.2013.05.039
70. Gratz LE, Keeler GJ, Marsik FJ, et al. Atmospheric transport of speciated mercury across southern Lake Michigan: Influence from emission sources in the Chicago/Gary urban area. Science of The Total Environment. 2013; 448: 84-95. doi: 10.1016/j.scitotenv.2012.08.076
71. Liu B, Keeler GJ, Timothy Dvonch J, et al. Urban-rural differences in atmospheric mercury speciation. Atmospheric Environment. 2010; 44(16): 2013-2023. doi: 10.1016/j.atmosenv.2010.02.012
72. Mao H, Talbot R. Speciated mercury at marine, coastal, and inland sites in New England – Part 1: Temporal variability. Atmospheric Chemistry and Physics. 2012; 12(11): 5099-5112. doi: 10.5194/acp-12-5099-2012
73. Manolopoulos H, Snyder DC, Schauer JJ, et al. Sources of Speciated Atmospheric Mercury at a Residential Neighborhood Impacted by Industrial Sources. Environmental Science & Technology. 2007; 41(16): 5626-5633. doi: 10.1021/es0700348
74. Choi HD, Huang J, Mondal S, et al. Variation in concentrations of three mercury (Hg) forms at a rural and a suburban site in New York State. Science of The Total Environment. 2013; 448: 96-106. doi: 10.1016/j.scitotenv.2012.08.052
75. Fostier AH, Michelazzo PAM. Gaseous and particulate atmospheric mercury concentrations in the Campinas Metropolitan Region (São Paulo State, Brazil). Journal of the Brazilian Chemical Society. 2006; 17(5): 886-894. doi: 10.1590/s0103-50532006000500011
76. Karuppasamy MB, Seshachalam S, Natesan U, Ramasamy K. Characterization of Atmospheric Mercury in the High-Altitude Background Station and Coastal Urban City in South Asia. In: Environmental Sustainability - Preparing for Tomorrow. IntechOpen; 2021.
77. Guo J, Ram K, Tripathee L, et al. Study on Mercury in PM10 at an Urban Site in the Central Indo-Gangetic Plain: Seasonal Variability and Influencing Factors. Aerosol and Air Quality Research. 2020; 20(12): 2729-2740. doi: 10.4209/aaqr.2019.12.0630
78. Koshle A, Pervez YF, Tiwari RP, Pervez S. Environmental pathways and distribution pattern of total mercury among soils and groundwater matrices around an integrated steel plant in India. Journal of Scientific & Industrial Research. 2008; 67:

523-530.
79. Supriti P, Mustala S, Asif Q. Mercury in soil around a 2,600 MW coal-fired super thermal power plant in India and Human Health Risk Assessment. Journal of Hazardous, Toxic, and Radioactive Waste. 2021; 25(3): 5021005.
80. Bhave P, Sadhwani K, Dhadwad M. Total mercury in soil and leachate from municipal solid waste dumping grounds in Mumbai, India. Environmental Earth Sciences. 2022; 81(1). doi: 10.1007/s12665-021-10156-0
81. Xiu GL, Jin Q, Zhang D, et al. Characterization of size-fractionated particulate mercury in Shanghai ambient air. Atmospheric Environment. 2005; 39(3): 419-427. doi: 10.1016/j.atmosenv.2004.09.046
82. Nguyen LSP, Sheu GR, Chang SC, et al. Effects of temperature and relative humidity on the partitioning of atmospheric oxidized mercury at a high-altitude mountain background site in Taiwan. Atmospheric Environment. 2021; 261: 118572. doi: 10.1016/j.atmosenv.2021.118572
83. Pankow JF. A simple box model for the annual cycle of partitioning of semi volatile organic compounds between the atmosphere and the earth's surface. Atmospheric Environment. 1993; 27: 1139-1152.
84. Lin CJ, Pehkonen SO. Two-phase model of mercury chemistry in the atmosphere. Atmospheric Environment. 1998; 32: 2543–2558.
85. Lin CJ, Pehkonen SO. Aqueous phase reactions of mercury with free radicals and chlorine: implications for atmospheric mercury chemistry. Chemosphere. 1999; 38: 1253–1263.
86. Subir M, Ariya PA, Dastoor AP. A review of uncertainties in atmospheric modeling of mercury chemistry I. Uncertainties in existing kinetic parameters – Fundamental limitations and the importance of heterogeneous chemistry. Atmospheric Environment. 2011; 45(32): 5664-5676. doi: 10.1016/j.atmosenv.2011.04.046
87. Zhang Y, Liu R, Wang Y, et al. Change characteristic of atmospheric particulate mercury during dust weather of spring in Qingdao, China. Atmospheric Environment. 2015; 102: 376-383. doi: 10.1016/j.atmosenv.2014.12.005
88. Kulshrestha UC, Reddy LAK, Satyanarayana J, et al. Real-time wet scavenging of major chemical constituents of aerosols and role of rain intensity in Indian region. Atmospheric Environment. 2009; 43(32): 5123-5127. doi: 10.1016/j.atmosenv.2009.07.025
89. Kulshrestha UC, Kumar N, Saxena A, et al. Identification of the nature and source of atmospheric aerosols near the Taj Mahal (India). Environmental Monitoring and Assessment. 1995; 34(1): 1-11. doi: 10.1007/bf00546242
90. Belis CA, Karagulian F, Larsen BR, et al. Critical review and meta-analysis of ambient particulate matter source apportionment using receptor models in Europe. Atmospheric Environment. 2013; 69: 94-108. doi: 10.1016/j.atmosenv.2012.11.009
91. Kulshrestha UC, Jain M, Sekar R, et al. Chemical characteristics and source apportionment of aerosols over Indian Ocean during INDOEX-1999. Current Science. 2001; 80 (10): 180-185.
92. Friedli HR, Radke LF, Lu JY, et al. Mercury emissions from burning of biomass from temperate North American forests: laboratory and airborne measurements. Atmospheric Environment. 2003; 37(2): 253–267.
93. Landis MS, Lewis CW, Stevens RK, et al. Ft. McHenry tunnel study: Source profiles and mercury emissions from diesel and gasoline powered vehicles. Atmospheric Environment. 2007; 41(38): 8711-8724. doi: 10.1016/j.atmosenv.2007.07.028
94. Mukherjee AB, Bhattacharya P, Sarkar A, Zevenhoven R. Mercury emissions from industrial sources in India and its effects in the environment. Springer, New York, USA; 2009. pp. 81–112.
95. Sharma SK, Mandal TK, Saxena M, et al. Variation of OC, EC, WSIC and trace metals of PM10 in Delhi, India. Journal of Atmospheric and Solar-Terrestrial Physics. 2014; 113: 10-22. doi: 10.1016/j.jastp.2014.02.008
96. Sharma SK, Mandal TK, Jain S, et al. Source Apportionment of PM2.5 in Delhi, India Using PMF Model. Bulletin of Environmental Contamination and Toxicology. 2016; 97(2): 286-293. doi: 10.1007/s00128-016-1836-1
97. Mishra M, Kulshrestha UC. Wet deposition of total dissolved nitrogen in Indo-Gangetic Plain (India). Environmental Science and Pollution Research. 2021; 29(6): 9282-9292. doi: 10.1007/s11356-021-16293-0
98. Rao MN, Latha R, Nikhil K, et al. Atmospheric gaseous mercury and associated health risk assessment in the economic capital of India. Environmental Monitoring and Assessment. 2024; 196(6). doi: 10.1007/s10661-024-12679-y